AD-A037 250 GENERAL ELECTRIC CO PHILADELPHIA PA SPACE DIV F/G 4/1
ATMOSPHERIC CLOUD PHYSICS LABORATORY (ACPL) OPTICAL MOTION CONT--ETC(U)
JAN 77 L R EATON, S L NESTE N00014-76-C-1057

UNCLASSIFIED NL

| OF |
AD
A037250

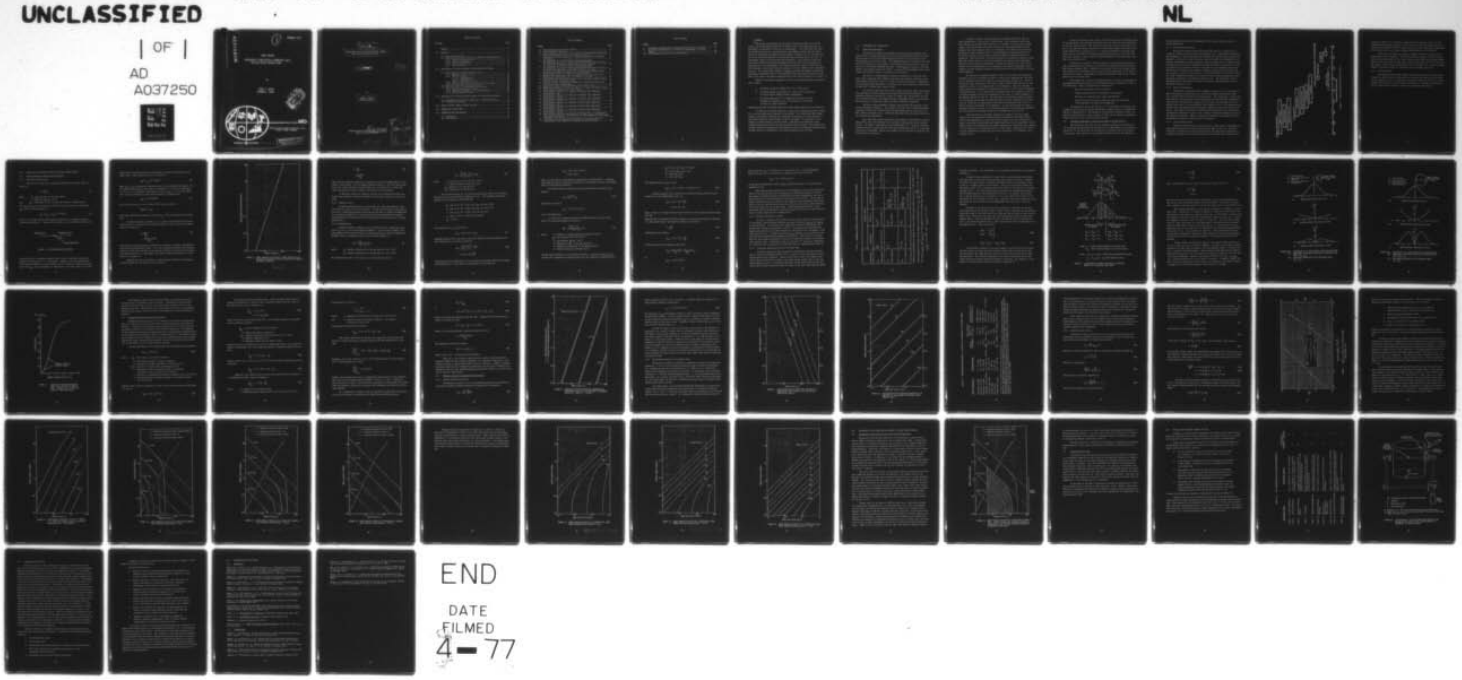

END

DATE
FILMED
4-77

FEBRUARY 1977

FINAL REPORT

ATMOSPHERIC CLOUD PHYSICS LABORATORY (ACPL) OPTICAL MOTION CONTROL STUDY

BY

LARRY R. EATON
SHERMAN L. NESTE

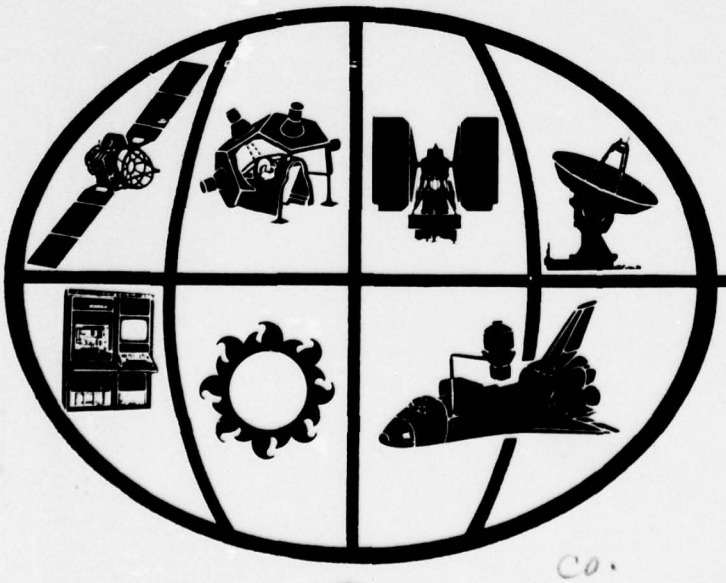

space division

PREPARED UNDER CONTRACT N00014-76-C-1057
OFFICE OF NAVAL RESEARCH

GENERAL ELECTRIC CO.
Space Div. Philadelphia, Pa

(9) FINAL REPORT,

(6) ATMOSPHERIC CLOUD PHYSICS LABORATORY (ACPL)
OPTICAL MOTION CONTROL STUDY,

(11) JAN [redacted] 77

(12) 58 P.

BY

(10) LARRY R. EATON
SHERMAN L. NESTE

(15) PREPARED UNDER CONTRACT N00014-76-C-1057
OFFICE OF NAVAL RESEARCH

405 025

TABLE OF CONTENTS

LIST OF FIGURES

LIST OF TABLES

SUMMARY

The concept of utilizing optical energy (radiation pressure) to provide motion control and stability for water droplets in the size range applicable to atmospheric cloud physics (5-100 μm) is investigated. It is shown that the inherent stabilizing forces of a gaussian laser beam (TEM_{00}) together with the beam's ability to manipulate individual particles makes a powerful tool for studying droplet or ice crystal growth and for initiating relative droplet motion in order to investigate various collision/coalescence phenomena. The utility of optical motion control (OMC) will be greatly enhanced with the advent of Shuttle/Spacelab payloads such as the Atmospheric Cloud Physics Laboratory (ACPL) in which the ambient opposing accelerations will be reduced to at least 1/1000 of that encountered on earth. This future ACPL capability together with current programs for developing shuttle compatible lasers in the 100-200 mW range will make it feasible to consider cloud physics experiments employing OMC on the earliest flights of the ACPL.

Specific experimental capability of OMC in the Shuttle/Spacelab environment will include:

1. Providing velocities ranging from 5 to < 0.01 cm/sec.
2. Providing precise positioning (± 5 μm) of water droplets up to 130 μm radius (droplet growth experiments).
3. Providing simulation of 1 g conditions (velocity or acceleration) for droplets up to ∿ 13 μm radius and fractional g levels for larger droplets.

Representative ACPL experiments which can utilize these capabilities are discussed.

In addition to the ACPL objective, a program for developing the OMC concept for use in an earth-based laboratory is presented. It is shown that OMC is applicable to experiments involving the coalescence efficiencies of cloud droplets in the growth transition region between 7 and 15 μm radius. In particular, the influence of droplet charge, electric fields, surfactants and turbulence on the collision/coalescence process in this size range can be studied. The proposed terrestrial laboratory program will also provide a means of evaluating and implementing the OMC concept for experiments in the Shuttle/Spacelab ACPL facility.

1.0 BACKGROUND AND INTRODUCTION

1.1 Past and Current Work

The growth of single cloud droplets and the interaction between cloud droplets has long been recognized as an area of investigation which must be pursued in order to more fully understand the formation of precipitation on the microphysical level (Eaton, 1971). The fundamental question is "How do the small drops (1-50 microns) in clouds grow, in the time period of one hour or less, to the size of rain drops (100-1000 microns)? A NASA sponsored facility, the Atmospheric Cloud Physics Laboratory (ACPL), is currently being designed with the objective of providing answers to questions of this nature.

The ACPL is a Shuttle/Spacelab payload consisting of a one meter wide double rack containing three chambers along with the equipment required to provide thermal and moisture control, as well as aerosol preparation, conditioning and characterization capability. Earth orbit will provide ambient accelerations of below 10^{-3} g (Final Report (ACPL), 1977).

The initial objectives are directed toward relatively simple cloud formation experiments involving primarily the warm cloud nucleation phenomena. This experiment selection was made as a result of taking into consideration the newness of experimentation in a weightless space environment which in turn dicated the selection of a relatively simple and better understood experiment.

The ACPL is being designed to permit future growth and expansion of the initial experiment cabability. The primary areas that have received the highest scientific priority are those dealing with scavenging and those involving ice. Some dynamic experiments (e.g., collision/coalescence) may also benefit from the low acceleration environment.

Most experiments beyond nucleation will require the observation of particles greater than a few micrometers for periods of time greater than a hundred seconds. The dynamic requirement of some experiments (i.e., relative velocities between droplets), coupled with the fact that the ACPL will not be in a true zero acceleration environment, dictate that methods will be required for position and motion control of droplets.

A number of motion control methods are available and many of them are being considered for "zero-gravity" applications. Each technique requires specific ambient and particle characteristics, for example: (a) acoustical methods require a gas (no-vacuum) environment and particle sizes approaching the wavelength of the sound (usually above one centimeter), (b) electrostatics and electrodynamics require charged bodies, (c) electromagnetics requires specific conductivity properties, and (d) optical methods require non-absorbing particle properties. The first three of the above operate on all particles within a volume while the fourth, optical, can be preferentially controlled so that individual particles can be uniquely manipulated. The physical properties of water and ice coupled with the requirements of the atmospheric microphysics experiments (both particle size and dynamics) indicate that optical motion control (OMC) is the most suited approach.

The concept of "radiation pressure" (not to be confused with radiometric pressure) was first introduced by Kepler in 1619 when he suggested that the pressure of sunlight caused comet tails to always point away form the sun. Until the relatively recent invention of the laser in 1960, radiation pressure was not considered as a force to be reckoned with in the laboratory. When the tremendous light intensities available from relatively low power ($\sim$ 0.1 W) lasers are applied to small particles ($\sim$ 10 μm radius) the resulting forces are competitive with the previously dominant ones such as radiometric forces (due to thermal gradients in the medium) and Earth's gravity. The feasibility of utilizing radiation pressure for controlling the movement of small particles is further enhanced by the potential for conducting the experiments in the nearly acceleration-free ($\sim 10^{-3}$ of Earth's gravity) environment of the Spacelab. In such surroundings the power requirements relative to those in a terrestrial laboratory can be greatly reduced or the size range of controllable drops can be extended (see Section 2.3).

The utilization of radiation pressure as a means of levitating small spheres has been successfully demonstrated in the laboratory by Ashkin (1970). In his first experiment, an argon laser with an output of a few milliwatts was used to accelerate micron-sized latex spheres which were freely suspended in water. Ashkin (1971) later demonstrated the stable levitation of transparent glass spheres ($\sim$ 20 μm diameter) in air and in vacuum ($\sim$ 1 Torr) using a laser beam of $\sim$ 250 mW. In other experiments a 50 mW laser was used to accelerate $\sim$ 5 μm diameter water droplets in air.

During his laboratory work, Ashkin (1970) discovered that the spheres used in his experiments were "simultaneously drawn into the beam axis and accelerated in the direction of light". The attraction toward the center of the beam is a result of the gaussian energy distribution across the beam diameter and will be discussed qualitatively in Section 2.1.4. It should be pointed out here that this effect will be very useful in maintaining the precise position of droplets since there will always be a force tending to keep the droplet in the beam center (similar to a potential well).

Utilization of optical radiation pressure to stably suspend small particles is presently being considered by a group at the Ruhr-Universität Bochum in West Germany (Schwem, 1976). Attempts to use magnetic forces to levitate individual particles for experiments on Mie scattering were complicated by the oscillation of the particles. Experiments are now being designed using a laser to more stably position the particles.

The capabilities of optical radiation pressure as a tool for studying the microphysical processes involved in the atmosphere must be evaluated in terms of the experiments. Typical questions to be answered are:

What are the droplet sizes of interest?

To what velocities must the droplets be accelerated?

What are the associated laser power requirements?

Are these power requirements compatible with the constraints of the laboratory (in the case of Spacelab)?

The approach of this study will be to: (1) investigate and evaluate the parameters which influence optical levitation or motion control, (2) define the limits of applicability to the Atmospheric Cloud Physics Laboratory (ACPL), (3) define an optical motion control concept for ACPL, and (4) outline a program for future work in the area of optical motion control.

1.2 Parameters Important to Optical Levitation or Motion Control

The efficiency with which optical radiation pressure can be applied to the levitation and positioning of particles will be determined by the characteristics of: (1) the particles, (2) the particle environment, and (3) the laser. In actuality, these factors are not mutually exclusive but for the purposes of

the following discussion their relationship to the present objective will be treated separately.

1.2.1 Particle Characteristics

The particle characteristics which obviously affect its amenability to levitation include its mass and optical properties (i.e., reflection, transmission and absorption). The particle mass will determine the applied force necessary to suspend or accelerate it while the optical characteristics will determine the efficiency with which the incident optical energy is converted into an applied force. It should be noted here that although all energy absorbed by the particle contributes directly to a momentum transfer to the particle, this absorbed energy also contributes to heating of the particle. Excessive heating of the particle will, in the case of a water droplet, increase its evaporation and if the heating results in a large temperature gradient in the particle the resulting photophoretic force may become comparable to the applied radiation force. The importance of these considerations, as they apply to optical levitation of water droplets, will be discussed in Section 2.1.2.

1.2.2 Particle Environment

The particle environment will be defined to consist of: (1) the medium in which the particle is being levitated, and (2) the ambient acceleration field (e.g., gravity) which is present in the laboratory. The temperature, pressure and viscosity are characteristics of the medium which will determine the thermophoretic forces acting on the particle (Section 2.1.2) as well as the maximum velocity a particle can attain for a given applied force (Section 2.3.3). The opposing acceleration field will determine the laser power required to perform the actual levitation. The results in Section 2.3 illustrate the requirements for conditions in a terrestrial laboratory as well as for a range of conditions expected to exist in the Spacelab on Shuttle. Figure 1 illustrates the sources and magnitudes of the perturbing acceleration fields expected for Spacelab.

1.2.3 Laser Characteristics

The laser characteristics, other than power, which must be considered include the efficiency of the laser and the optical mode of the beam. The laser efficiency is normally not the controlling factor for experiments conducted in a terrestrial laboratory since laser input power and physical size are usually not

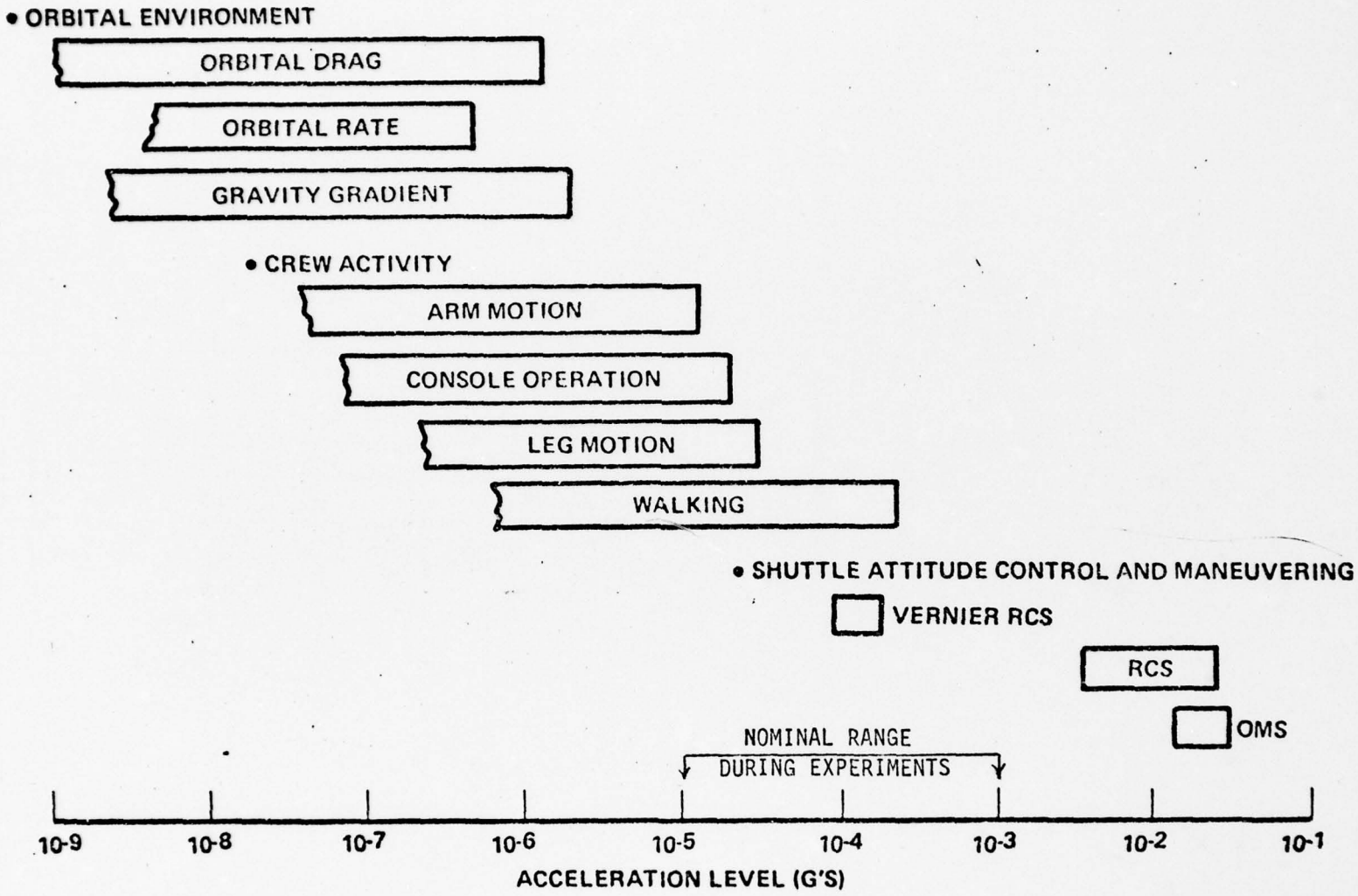

FIGURE 1. SHUTTLE/SPACELAB ACCELERATION LEVELS

a problem. However, for experiments conducted in the Spacelab, power and size requirements may become important. Since the actual output wavelength has little effect on the required levitation power (Section 2.3.3) an important consideration in choosing a laser (e.g., Argon vs Helium-Neon) should be its efficiency.

Selection of the beam mode (TEM_{01} or TEM_{00}) is dictated largely by the requirements of the experiment. Askin (1974) has successfully levitated spheres using both the TEM_{01} mode (do-nut shaped beam) and the TEM_{00} mode (gaussian beam). His data shows that with the TEM_{00} mode, spherical particles can be levitated much more stably. Since precise positioning is one of the objectives of optical motion control, the obvious choice for consideration is the TEM_{00} mode laser.

1.2.4 Analysis Method

The analyses which follow evaluate the importance of the above parameters relevant to the objective of levitating (positioning) and controlling the motion of water droplets in air. Consequently the detailed examples which are presented reflect this objective, and will provide guidelines for assessing the applicability of optical motion control to problems in atmospheric microphysics.

2.0 EVALUATION OF CRITICAL FACTORS FOR OPTICAL MOTION CONTROL

2.1 Forces Relevant to Optical Motion Control

2.1.1 Radiation Pressure Forces

The force on a body due to radiation pressure (van de Hulst, 1957) is given by:

$$F = \frac{W}{c} Q_{pr} \tag{1}$$

where: W = power incident on the body (watts)

c = speed of light (cm sec^{-1})

and Q_{pr} = efficiency factor for radiation pressure (dimensionless)

The value of Q_{pr} can be calculated from the efficiency factors for absorption Q_{abs} and for scattering Q_{sca} as:

$$Q_{pr} = Q_{abs} + Q_{sca} \overline{(1 - \cos \theta)} \tag{2}$$

where θ is the angle between the scattered light and the transmitted light as illustrated in Figure 2. Equation (2) indicates that all absorbed radiation contributes directly to momentum transfer, while only the backward components of scattered radiation ($\cos \theta = -1$) contribute. However, the calculations which follow pertain primarily to water droplets in air so that the radiation pressure due to the Q_{abs} term is negligible in comparison to the other terms, i.e., water

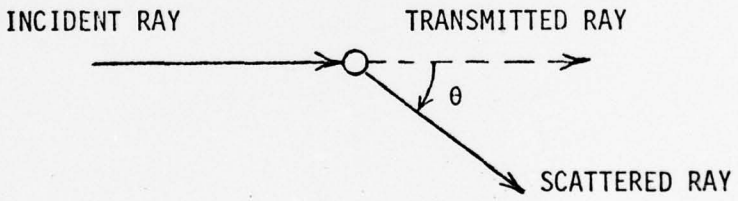

FIGURE 2. SCATTERING ANGLE DEFINITION

droplets are considered essentially transparent at visible wavelengths (van de Hulst, 1957). Thus, Equation (2) can be written as:

$$Q_{pr} = Q_{sca} \overline{(1 - \cos \theta)} \tag{3}$$

where $Q_{sca} = Q_{ext}$ (extinction efficiency factor) for a non-absorbing sphere. For the case of water droplets with index of refraction m = 1.33 and size parameter $x = 2\pi r/\lambda >> 1$, van de Hulst (1957) gives a value of $Q_{ext} = 2$ (r is drop radius and λ is light wavelength in same units). Equation (3) now becomes:

$$Q_{pr} = 2 \overline{(1 - \cos \theta)} \tag{4}$$

For the above value of m, van de Hulst (1957) gives a value of:

$$\overline{(\cos \theta)} = 0.87$$

which when substituted in Equation (4) gives $Q_{pr} = 0.26$ for spherical water droplets.

The power required to levitate, *i.e.*, exactly counterbalance the gravitational force on a water droplet is given by setting F = mg in equation (1) which then can be written as:

$$W = \frac{mg\ c}{Q_{pr}} = \frac{4/3\ \pi\ \rho\ r^3\ gc}{Q_{pr}} \tag{5}$$

which gives the levitation power required for a particle of radius r and density ρ in the earth's gravitational field. For a 10 μm (radius) spherical water droplet, a power of 0.047 watts incident on the particle surface is required for levitation. The required power for g = 980 cm/sec^2 (at earth's surface) is plotted as a function of r in Figure 3.

Equation (5) can be converted to a power density (watts/cm^2) requirement by merely dividing by the particle area to obtain:

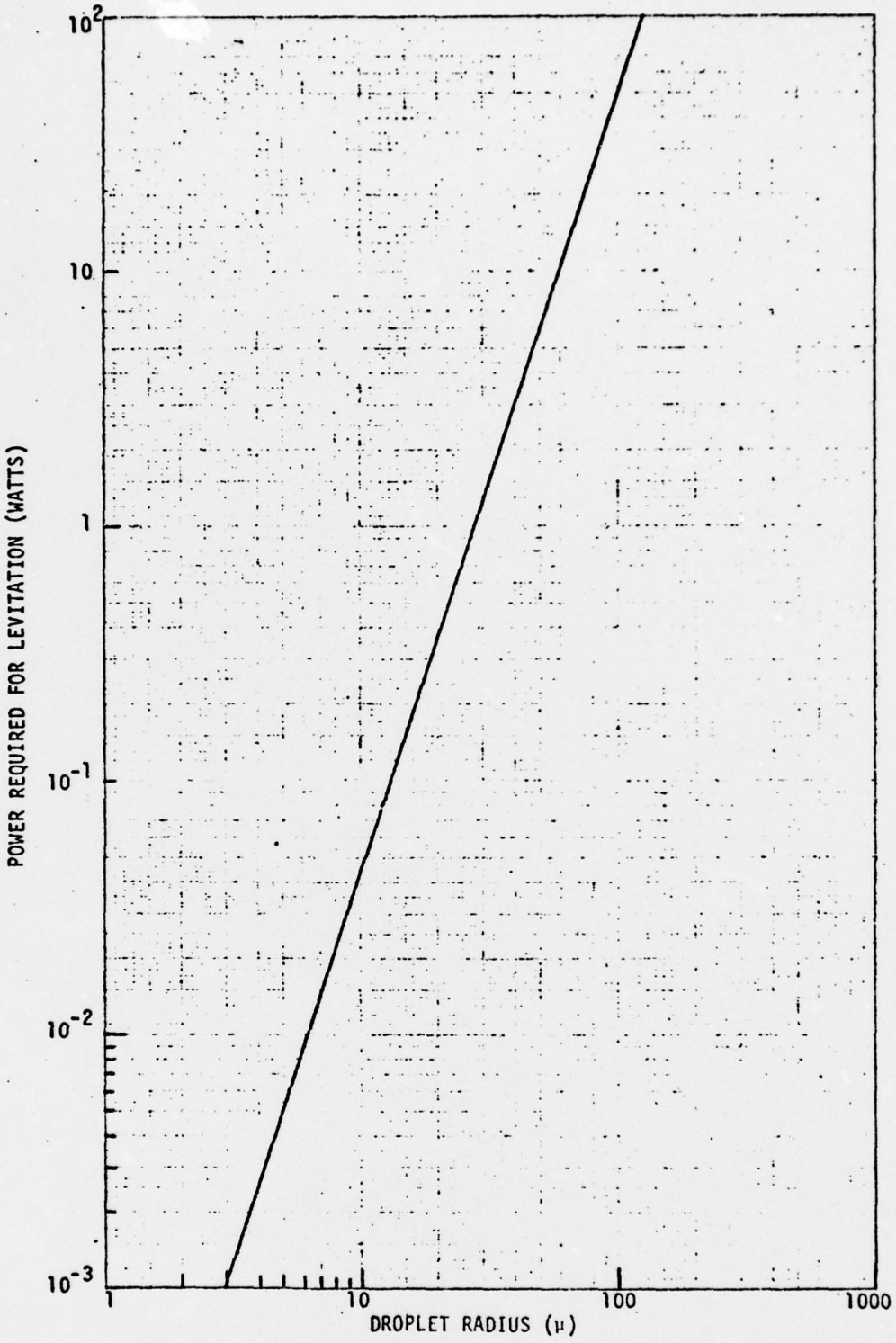

FIGURE 3. POWER REQUIRED TO LEVITATE A WATER DROPLET IN AN OPPOSING ACCELERATION FIELD OF 980 CM/SEC^2 (GRAVITY AT EARTH'S SURFACE).

$$I = \frac{W}{\pi r^2} \qquad (6)$$

$$= \frac{4\ \rho\ r\ g_c}{3\ Q_{pr}}$$

Thus, the beam intensity required for levitation is directly proportional to the radius of the droplet. For the example evaluated above ($r = 10^{-3}$ cm), this translates into a power density of approximately 1.5×10^4 watts/cm^2, or about 10^5 times the intensity of solar energy on the earth (~ 0.14 watts/cm^2).

It should be noted that equations (5) and (6) are general and can be applied to any particle for which the proper value for Q_{pr} is known or can be computed.

2.1.2 Phoretic Forces

A temperature difference over the surface of a body surrounded by a gas will result in a net force on the particle. If the uneven heating of the particle is due to a temperature gradient within the gas the force is called thermophoretic. If a one-sided illumination of the particle and resulting absorption causes an uneven temperature distribution within the particle the resulting force is called photophoretic.

2.1.2.1 Thermophoretic

Consider a sphere residing in a gas in which there is a temperature gradient ∇T_g (e.g., in a thermal diffusion chamber). If the particle radius (r) is much greater than the mean free paths of the gas molecules, then the temperature gradient within the spherical body is given by Fuchs (1964) as:

$$\nabla T_p = \frac{3\ k_g}{2\ k_g + k_p} (\nabla T_g) \qquad (7)$$

where: k_g = thermal conductivity of the gas (erg cm^{-1} sec^{-1} °K^{-1})

k_p = thermal conductivity of the gas (erg cm^{-1} sec^{-1} °K^{-1})

The thermophoretic force on the particle is then given by Fuchs as:

$$F_{th} = \frac{9\ \pi\ k_g}{2k_g + k_p} \frac{\eta^2\ r}{\rho_g\ T_g} (\nabla Tg) \qquad (8)$$

where: η = viscosity of the gas (gm cm^{-1} sec^{-1})

r = radius of spherical particle (cm)

ρ_g = density of the gas (gm cm^{-3})

T_g = temperature of the gas (°K)

The calculated value for F_{th} below illustrates the effect of the thermophoretic force on a water droplet suspended in air. The following values were assumed for the parameters in Equation (8):

k_g (air at 21 °C) = 2.56×10^3 ergs cm^{-1}-sec^{-1}-$°K^{-1}$

k_p (H_2O at 21 °C) = 5.95×10^4 ergs cm^{-1}-sec^{-1}-$°K^{-1}$

η (air at 21 °C) = 1.838×10^{-4} gm cm^{-1} sec^{-1}

ρ_g (air at 21 °C) = 1.201×10^{-3} gm cm^{-3}

T_g = 294 °K

The expression for F_{th} then becomes:

$$F_{th} = 1.07 \times 10^{-7}\ r\ \nabla T_g \qquad (9)$$

Dividing equation (9) by the mass of the water droplet yields an expression for the thermophoretic acceleration given by:

$$a_{th} = \frac{1.07 \times 10^{-7}\ r\ \nabla T_g}{4/3\ \pi\ \rho\ r^3} \qquad (10)$$

$$= 2.55 \times 10^{-8} \frac{\nabla T_g}{r^2}$$

Evaluating the above expression for a 10 micron water droplet radius and a temperature gradient of 1 °K/cm yields a thermophoretic acceleration of

$$a_{th} = 2.55 \times 10^{-2} \text{ cm sec}^{-2}$$
$$= 2.6 \times 10^{-5} \text{ g}$$

where g is the earth's gravitational acceleration of the 980 cm/sec . Equation (10) indicates that the temperature gradients in the medium will have the greatest effect on the smallest particles.

The Stokes velocity associated with this acceleration is given by the formula:

$$v_{th} = \frac{2}{9} \frac{\rho r^2}{\eta} a_{th} \tag{11}$$

which gives a value of

$$v_{th} = 3.1 \times 10^{-5} \text{ cm sec}^{-1}$$

2.2.2.2 Photophoretics

In the case of aspherical particle illuminated from one side, Fuchs gives the resulting photophoretic force as:

$$F_{ph} = \frac{-3\pi \eta^2 r R_g}{2 PM (k_g + k_p)} I\alpha \ell \tag{12}$$

where:
- I = density of luminous energy flux (erg cm^{-2} sec^{-1})
- R_g = gas constant (ergs $^{\circ}K^{-1}$ $mole^{-1}$)
- P = gas pressure (gm cm^{-1} sec^{-2})
- M = molecular weight of the gas (gm $mole^{-1}$)
- α = absorption coefficient of the particle (cm^{-1})
- ℓ = optical absorption thickness (cm^{-1})

and all other parameters are as previously defined. A typical value of F_{ph} is calculated by assuming the following values for the parameters in Equation (12):

$$R_g = 8.317 \times 10^7 \text{ ergs } ^\circ C^{-1} \text{ mole}^{-1}$$

$$P = 1.10 \times 10^6 \text{ gm cm}^{-1} \text{ sec}^{-2}$$

$$M = 28.96 \text{ gm mole}^{-1}$$

$$\alpha = 2.9 \times 10^{-3} \text{ cm}^{-1}$$

The computed value for F_{ph} is then:

$$F_{ph} = -2.11 \times 10^{-14} \; r \; I \; \ell \text{ gm-cm sec}^{-2} \tag{13}$$

Dividing equation (13) by the mass of the water droplet gives the acceleration due to the photophoretic force as:

$$a_{ph} = -5.1 \times 10^{-15} \frac{I \ell}{r^2} \tag{14}$$

$$= -1.0 \times 10^{-14} \frac{I}{r}$$

where a value of 2r (worst case) has been assumed for the optical absorption thickness (ℓ).

Assuming that the incident levitation power W as calculated previously is focussed to a beam width equal to the particle diameter we can write:

$$I = \frac{W}{\pi r^2} \tag{15}$$

and Equation (14) becomes:

$$a_{ph} = -1.0 \times 10^{-14} \frac{W}{\pi r^3} \tag{16}$$

Substituting from W from Equation (5) gives:

$$a_{ph} = \frac{1.0 \times 10^{-14}}{\pi r^3} \; \frac{4/3 \; \pi \; \rho \; r^3}{Q_{pr}} \; gc \tag{17}$$

or

$$a_{ph} = -1.54 \times 10^{-3} \; g$$

which shows that a_{ph} is independent of the particle size. The corresponding Stokes velocity for a 10 μ radius water droplet in air has a value of:

$$v_{ph} = -1.8 \times 10^{-3} \text{ cm sec}^{-1}$$

In the above computations we have assumed conditions relevant to a water droplet suspended in air.

The negative sign associated with the photophoretic force and acceleration indicate that the particle will be propelled in a direction opposite to that of the incident radiation (negative photophoresis) whereas thermophoretic and radiation pressures are in the direction of the beam for water in air. In the case of nearly transparent particles (such as water droplets) this phenomenon results from the fact that the rays refracted inside the particle will cause a greater heating on the side away from the incident light. Highly absorbing particles, on the other hand, will be heated more on the front surface and be moved in the direction of the incident light (positive photophoresis).

2.1.3 Relative Importance of Forces

In order to evaluate the influence of the phoretic forces on the objective of levitating a particle using radiation pressure, the ratios a_{ph}/a_{pr} and a_{th}/a_{pr} can be calculated. To facilitate this computation the factors upon which each acceleration depends are presented in Table I. The groupings are determined by whether the parameters are characteristics of the particle, the environment or the laser (Section 1.2). It should be noted that a_{ph} depends on a_{pr} by virtue of the fact that the particle heating depends directly on W. Thus it can be concluded that for this example the phoretic forces can be neglected compared to the radiation pressure force. Furthermore, since a_{th} varies as r^{-2} and a_{ph} is independent of r they will not be important for larger droplets (cf. example bottom Table I).

2.1.4 Transverse Stabilizing Force of the Laser Beam

The forces which have been discussed in the previous sections are important in terms of determining whether or not a particle can be levitated or accelerated using optical radiation. However, given that a laser will suspend a particle, why does the particle remain in the beam and not slowly drift to the side and subsequently fall? As previously mentioned, Ashkin (1970) observed that particles were actually attracted toward the center of the laser beam (gaussian mode)

TABLE I. PARAMETERS AFFECTING VARIOUS ACCELERATION FORCES ON A PARTICLE

Acceleration	Relevant Factor			
	Multiplier	Particle	Environment	Laser
a_{pr} (980 cm/sec^2)	$\frac{3}{4\pi c}$ (8×10^{-12} sec cm^{-1})	$Q_{pr}/\rho r^3$ (2.6×10^{8} gm^{-1})	1	W (4.7×10^{5} erg/sec)
a_{th} (0.03 cm/sec^2)	27/4	$1/\rho r^2$ (10^{6} cm gm^{-1})	$\frac{k_g \eta^2 \nabla T_g}{(2k_g + k_p)\rho_g T_g}$ (3.8×10^{-9} gm sec^{-2})	1
a_{ph} (-1.5 cm/sec^2)	$-3\, c a_{pr}$ (-8.8×10^{13} cm^2 sec^{-3})	α/Q_{pr} (1.1×10^{-2} cm^{-1})	$\frac{\eta^2 R_g}{pM(k_g + k_p)}$ (1.6×10^{-12} sec)	1

Numbers in parentheses are values for a 10 μm (radius) water droplet in air at T = 294 °K and P = 1 atm. Each acceleration is given by the product of the factors (e.g., $a_{pr} = \frac{3}{4\pi c} \times \frac{Q_{pr}}{\rho r^3} \times 1 \times W$). Calculating the ratios a_{ph}/a_{pr} and a_{th}/a_{pr} for the example of a 10 μm radius water droplet in air we find:

$$a_{ph}/a_{pr} = 1.5 \times 10^{-3} \quad \text{and} \quad a_{th}/a_{pr} = 3.1 \times 10^{-5}.$$

and held in position. This phenomenon can be explained qualitatively by referring to Figure 4.

A droplet being suspended by a laser with a gaussian energy distribution will experience a variation in the incident energy across its surface. Consider the sketch of Figure 4 which illustrates the optical paths of two parallel rays, I_1 and I_2, of light incident on the droplet. Both rays are equally distant from the droplet center but I_1 originates nearer the center of the beam and is therefore stronger than I_2. The forces resulting on the droplet are determined by drawing the resulting vectors at each droplet-air interface. For example, the incident ray I_1 and the reflected ray I_{1D} produce a force F_{1Ri}, while the incident ray and the refracted ray I_{1R} produce a force F_{1Di}. Similarly, the forces resulting at the exit point of ray I_i as well as the corresponding forces for ray I_2 can be determined.

As shown in the sketch, all forces contribute to "pushing" the particle in the direction of the incident light. However, forces F_{1Di} and F_{1Do} are directed toward the center of the beam while forces F_{2Di} and F_{2Do} are directed away from the beam center. The forces, F_{1Ri} and F_{1Ro}, and F_{2Ri} and F_{2Ro} cancel to first order (Ashkin, 1970). Since the intensity of ray I_1 is greater than the intensity of ray I_2, all forces associated with I_1 will be greater than the corresponding forces associated with I_2. Thus we can write:

$$\left.\begin{aligned} F_{1Di} &> F_{2Di} \\ F_{1Do} &> F_{2Do} \end{aligned}\right\} \tag{18}$$

or

$$F_{1Di} + F_{1Do} > F_{2Di} + F_{2Do} \tag{19}$$

As was shown in Figure 4, all rays incident on the left hand of the droplet will result in a force directed toward the beam center (-x direction) while rays incident on the right half will result in a force directed out of the beam (+x direction). The relative magnitudes of all rays can be determined by their origin within the gaussian energy distribution of the beam. For example, I_1 originates at the beam center (x=0) and will have a magnitude of:

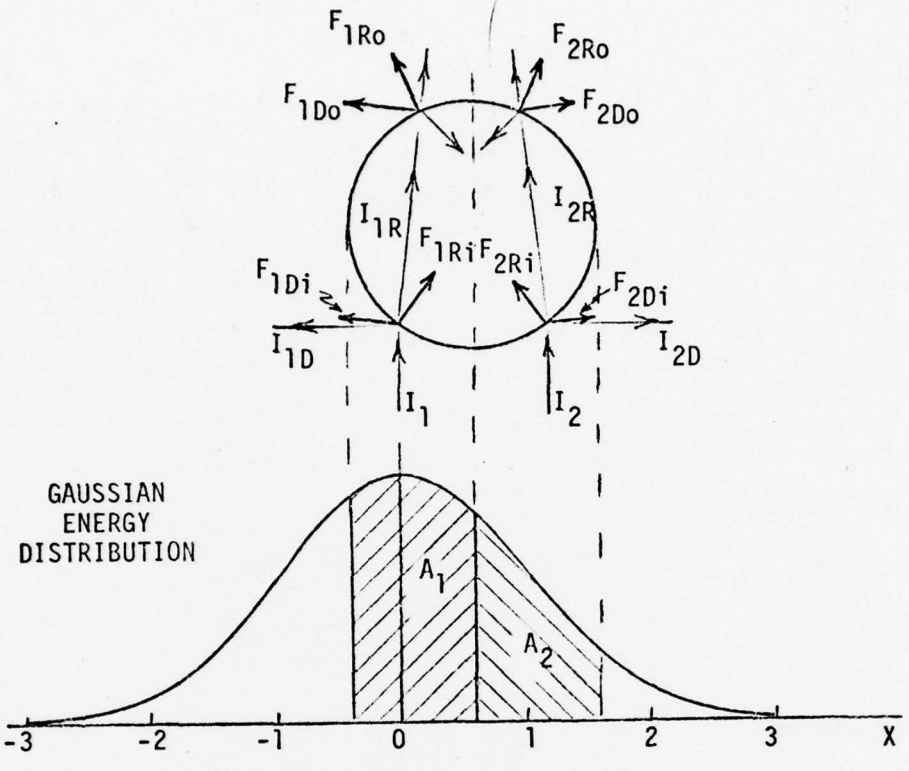

FORCES ON LEFT SIDE OF DROPLET	FORCES ON RIGHT SIDE OF DROPLET
$F_{1Ri} + F_{1Ro} \simeq 0$	$F_{2Ri} + F_{2Ro} \simeq 0$
$F_{1Di} + F_{1Do} = f_{x-}$	$F_{2Di} + F_{2Do} = f_{x+}$
$F_{x-} = \Sigma f_{x-} \propto A_1$	$F_{x+} = \Sigma f_{x+} \propto A_2$

where F_{x-} = force pushing droplet into beam center

F_{x+} = force pushing droplet out of beam center

Note: $F_{x-}/F_{x+} \propto A_1/A_2$ = Restoring Force/Repelling Force

$F_{x-} - F_{x+} \propto A_1 - A_2$ = Net Restoring Force

FIGURE 4. ILLUSTRATION OF FORCES ACTING ON A SPHERICAL DROPLET BY A GAUSSIAN LASER BEAM

$$I_1 \propto \frac{e^{-x}}{\sqrt{2\pi}} \tag{20}$$

$$\approx 0.4$$

while I_2 originates at the 2σ point (x=1) and will have a value of:

$$I_2 \propto \frac{e^{-1}}{\sqrt{2\pi}} \tag{21}$$

$$\approx 0.15$$

However, the total restoring force on the droplet (F_{x-}) will be proportional to the area A_1 under the gaussian energy distribution curve. Similarly, the total force tending to push the droplet out of the beam (F_{x+}) will be proportional to A_2.

The relative magnitudes of these forces can easily be computed for various drop sizes. In Figure 5a, a droplet of diameter 1σ (relative to the width of the laser beam) is positioned in a gaussian laser beam. As the droplet is moved across the diameter of the laser beam, the corresponding values of F_{x-}/F_{x+} (i.e., A_1/A_2) are computed in relative units and plotted in Figure 5b. The ratio has a minimum value of 1 when the droplet is at the beam center, and increases as the droplet moves to either side of center, indicating that F_{x-} is always greater than F_{x+}. Similarly, the net restoring force (-x direction) can be determined qualitatively from a plot of $(F_{x-} - F_{x+})$ as shown in Figure 5c. The maximum restoring force occurs when the droplet is centered at the 1σ position of the beam corresponding to the point at which the intensity gradient of the gaussian distribution is a maximum.

Similar results are plotted in Figure 6 for a droplet whose diameter is 2σ (i.e., twice as large as the above example). As shown in that figure, which is plotted to the same scale as Figure 5, the corresponding values of (F_{x-}/F_{x+}) and $(F_{x-} - F_{x+})$ have increased greatly. These results provide qualitative indication that the restoring force on a particle will increase as the droplet size and beam size become comparable. Figure 7 illustrates this effect for $(F_{x-} - F_{x+})_{max}$, i.e., a droplet positioned at the 1σ point in the beam. It should be noted, however, that the restoring force will become less effective as the droplet becomes so large that it effectively presents a flat surface to the beam.

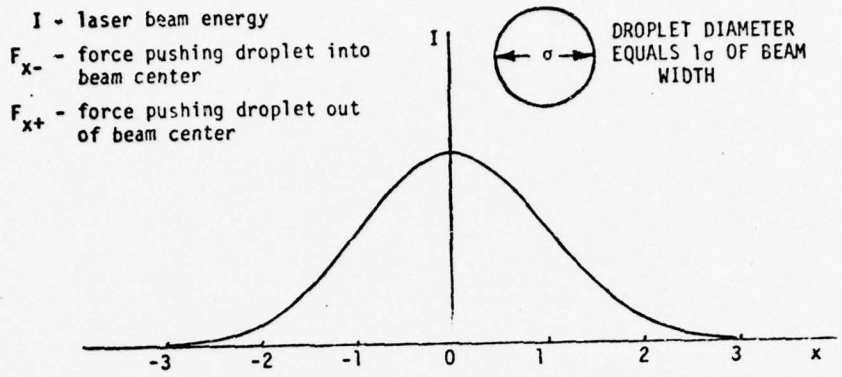

5a. DISTANCE FROM BEAM CENTER (UNITS OF σ)

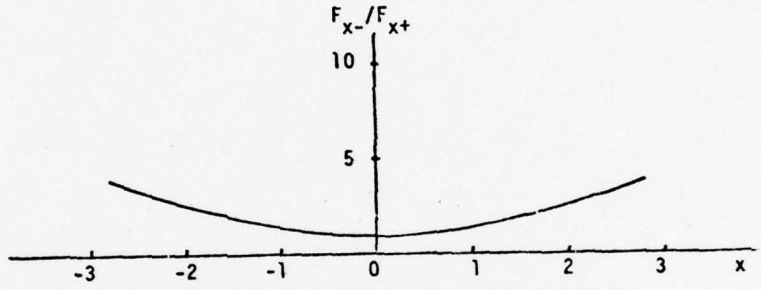

5b. POSITION OF DROPLET CENTER RELATIVE TO BEAM

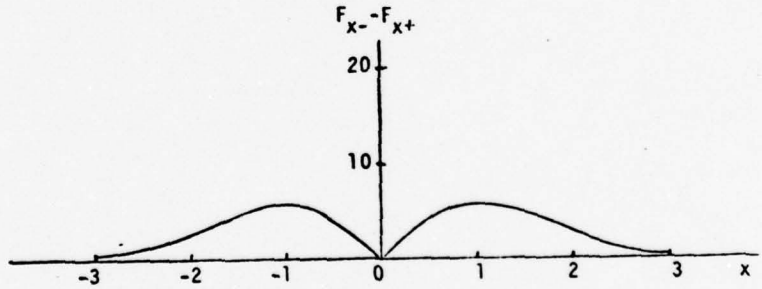

5c. POSITION OF DROPLET CENTER RELATIVE TO BEAM

FIGURE 5(a). COMPARISON OF 1σ WATER DROPLET WITH GAUSSIAN BEAM.
(b). POSITIONAL VARIATION OF RESTORING FORCE/REPELLING FORCE (F_{x-}/F_{x+}).
(c). POSITIONAL VARIATION OF NET RESTORING FORCE ($F_{x-}-F_{x+}$).

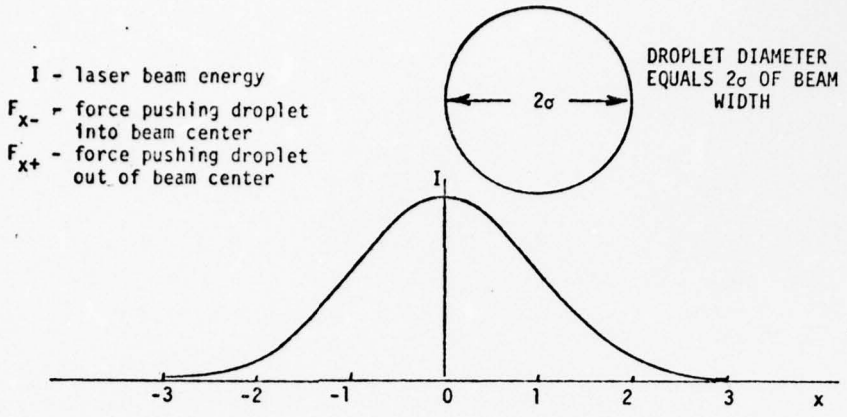

6a. DISTANCE FROM BEAM CENTER (UNITS OF σ)

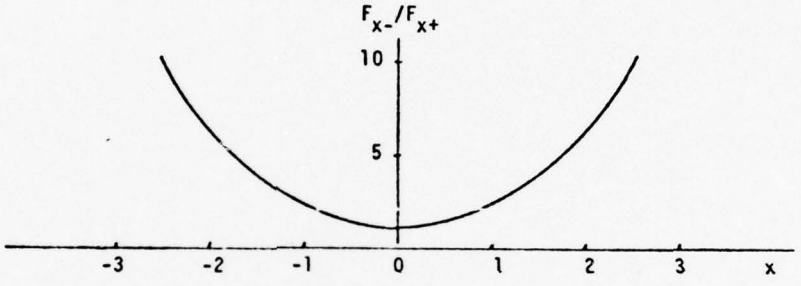

6b. POSITION OF DROPLET CENTER RELATIVE TO BEAM

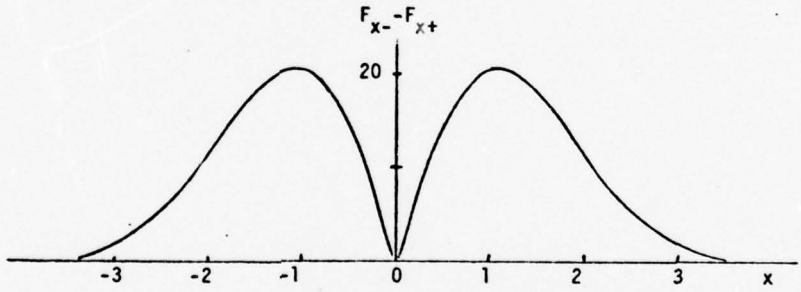

6c. POSITION OF DROPLET CENTER RELATIVE TO BEAM

FIGURE 6(a). COMPARISON OF 2σ WATER DROPLET WITH GAUSSIAN BEAM.
(b). POSITIONAL VARIATION OF RESTORING FORCE/REPELLING FORCE (F_{x-}/F_{x+}).
(c). POSITIONAL VARIATION OF NET RESTORING FORCE ($F_{x-}-F_{x+}$).

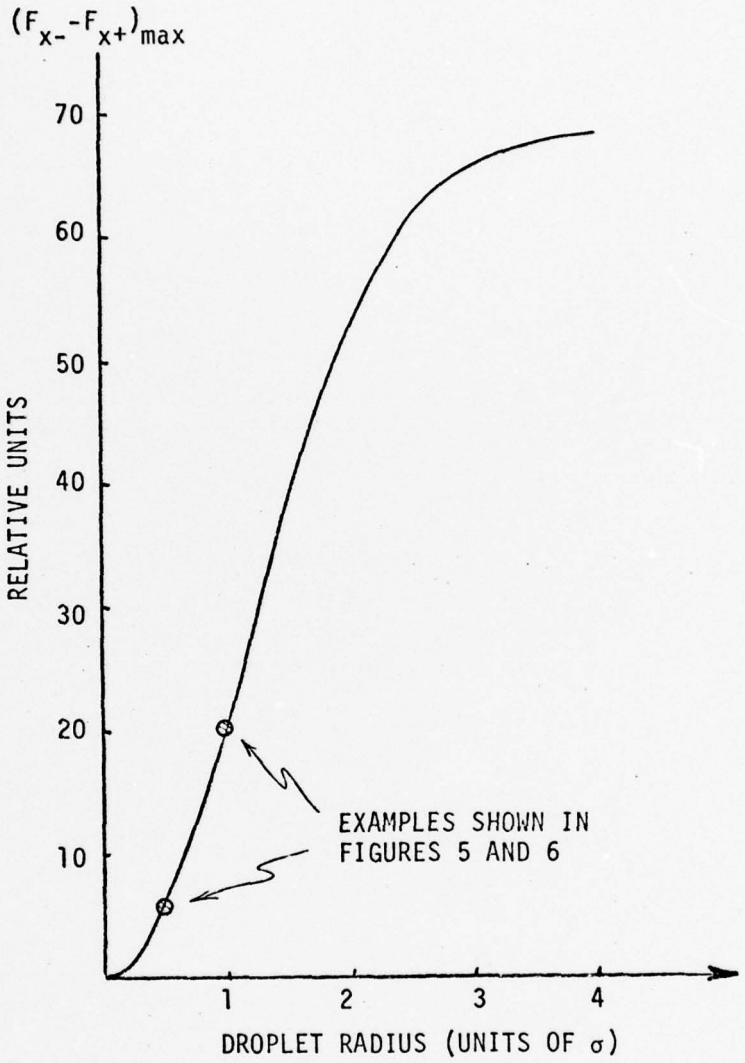

FIGURE 7. VARIATION OF MAXIMUM RESTORING FORCE AS A FUNCTION OF DROPLET SIZE. DROPLET SIZE IS GIVEN IN TERMS OF LASER BEAM WIDTH.

The foregoing results indicate the importance of minimizing the size of the laser beam as it impinges upon the droplet. In addition to providing the greatest levitation force, it will also maximize the "trapping" effect of the gaussian laser beam. This last effect is very important in terms of stabilizing a body and will enhance the use of optical radiation for precise positioning of droplets.

2.2 Heating of Optically Levitated Particles

Consideration must be given to the heating of an optically levitated particle in as much as it may define the limits within which optical levitation is feasible. A fraction of the incident optical energy will be converted into thermal energy, resulting in an increase of the droplet temperature. The magnitude of this temperature increase will depend primarily on the physical characteristics of the droplet and the medium in which it is being levitated. The eventual steady-state temperature can be computed in a relatively straightforward manner by equating the heat input (absorbed optical energy) and heat loss (radiation and conduction to the medium) for the levitation power required.

The heat equivalent of the incident beam can be expressed by the equation:

$$\dot{Q}_{in} = \alpha\, k(1-q)\, W \tag{22}$$

where: $\dot{Q}_{in}$ = heat input to the droplet (cal/sec)

W = total power incident on droplet (ergs/sec)

q = fraction of incident beam which is reflected ($\simeq 0.1$)

$(1-q)$ = fraction of incident beam transmitting ($\simeq 0.9$)

k = conversion factor from optical energy to mechanical equivalent of heat ($\simeq 0.239 \times 10^{-7}$ cal/erg)

α = fraction of transmitted beam which is absorbed $(2.9 \times 10^{-3}\ \text{cm}^{-1})\ell$

ℓ = optical absorption thickness (assume $\simeq 2r$, diameter of drop as a worst case)

Equation (22) can thus be expressed in terms of the levitation power and the droplet size as:

$$\dot{Q}_{in} = 1.25 \times 10^{-10}\, Wr \tag{23}$$

As previously stated the droplet will, given sufficient time, attain an equilibrium temperature at which the heat conduction outward from the center of the spherical drop can be expresses as:

$$\dot{Q}_{c_{out}} = -k_g A \, dT/dr \tag{24}$$

$$= -4\pi r^2 k_g \, dT/dr$$

which will be true for any drop radius (r). In the above expression the parameters are defined as follows:

$\dot{Q}_{c_{out}}$ = rate of outward heat flow (cal/sec)

r = radius from center of drop (cm)

k_g = thermal conductivity of media (erg cm^{-1} sec^{-1} $°K^{-1}$)

T = absolute temperature (°K)

A = spherical surface area at radius r (cm^2)

Equation (24) can be integrated to obtain the outward heat flow from the spherical surface at Temperature T_s to the conductive medium at temperature T_m with the result:

$$\dot{Q}_{c_{out}} = 4\pi r k_g (T_s - T_m) \tag{25}$$

Using a value of 6.1×10^{-5} cal cm^{-1} sec^{-1} $°K^{-1}$ for the thermal conductivity of air we obtain:

$$\dot{Q}_{c_{out}} = 7.7 \times 10^{-4} r (T_s - T_m) \tag{26}$$

Similarly, the radiative heat loss from the droplet can be calculated in a straightforward manner using the equation:

$$\dot{Q}_{r_{out}} = \varepsilon \sigma (T_s^4 - T_m^4) \tag{27}$$

where: ε = emissivity of the water droplet

σ = Stephen-Boltzman constant (1.36×10^{-12} cal sec^{-1} cm^{-2} $°K^{-4}$)

The emissivity is given by:

$$\epsilon = 1 - e^{-\alpha \ell} \tag{28}$$
$$\simeq \alpha \ell \text{ for } \alpha \ell << 1$$

where: α = absorption coefficient of the drop (2.9×10^{-3} cm^{-1} ℓ)

and ℓ = optical absorption thickness (assume $\ell \simeq 2r$, diameter of drop as a worst case)

Substitution into Equation (6) yields:

$$\dot{Q}_{r_{out}} = 7.9 \times 10^{-15} \, r \, (T_s^4 - T_m^4) \tag{29}$$

The relative importance of radiative and conductive heat loss from the droplet is readily obtained by dividing Equation (25) into Equation (29) to obtain:

$$\left(\frac{\dot{Q}_r}{\dot{Q}_c}\right)_{out} = 10^{-11} \, (T_s^3 + T_s^2 \, T_m + T_s \, T_m^2 + T_m^3) \tag{30}$$

Assuming a worst case condition of T_s = 373 °K (boiling point of water) and T_m = 294 °K (room temperature) we find:

$$\left(\frac{\dot{Q}_r}{\dot{Q}_c}\right)_{out} \simeq 1.5 \times 10^{-3}.$$

Clearly, the radiative heat loss is insignificant when compared to the conductive heat loss to the surrounding medium (assumed to be air at 1 atm). However, it must be pointed out that if the levitation is attempted at successively lower pressures the conductive effects will decrease until eventually the radiative term becomes dominant.

As a consequence of Equation (30) the equilibrium temperature of the droplet can be calculated by considering the simplifed heat balance equation:

$$\dot{Q}_{in} = \dot{Q}_{c_{out}} \tag{31}$$

or

$$1.25 \times 10^{-10} \text{ Wr} = 7.7 \times 10^{-4} \text{ r } (T_s - T_m) \tag{32}$$

which is obtained from Equations (23) and (26). Solving for the temperature increase of the drop we have:

$$\Delta T = (T_s - T_m) = 1.6 \times 10^{-7} \text{ W} \tag{33}$$

where W (the levitation power) is given by Equation (5) as:

$$W = \frac{4/3 \ \pi \ \rho \ r^3 \ gc}{Q_{pr}}$$

The temperature delta then becomes:

$$\Delta T = 7.7 \times 10^{4} \text{ g } r^3 \tag{34}$$

where a value of $\rho = 1$ (water) has been assumed.

Thus, for a 10 μm (radius) spherical water droplet, being levitated at standard temperature and pressure conditions, in a terrestial laboratory, a temperature increase of approximately 0.08 °C will be observed. A graph of required levitation power and the corresponding temperature rise is given in Figure 8 as a function of particle size assuming opposing acceleration fields of 1 g, 10^{-3} g and 10^{-6} g, where g = 980 cm/sec^2.

2.3 Practical Limits of Acceleration and Velocity

2.3.1 Typical Acceleration Levels

As discussed in Section 2.1.3, the acceleration which can be imparted to a particle by optical radiation pressure is expressed by the equation:

$$a_{pr} = \frac{3}{4c\pi} \ \frac{Q_{pr}}{pr^3} \ W. \tag{35}$$

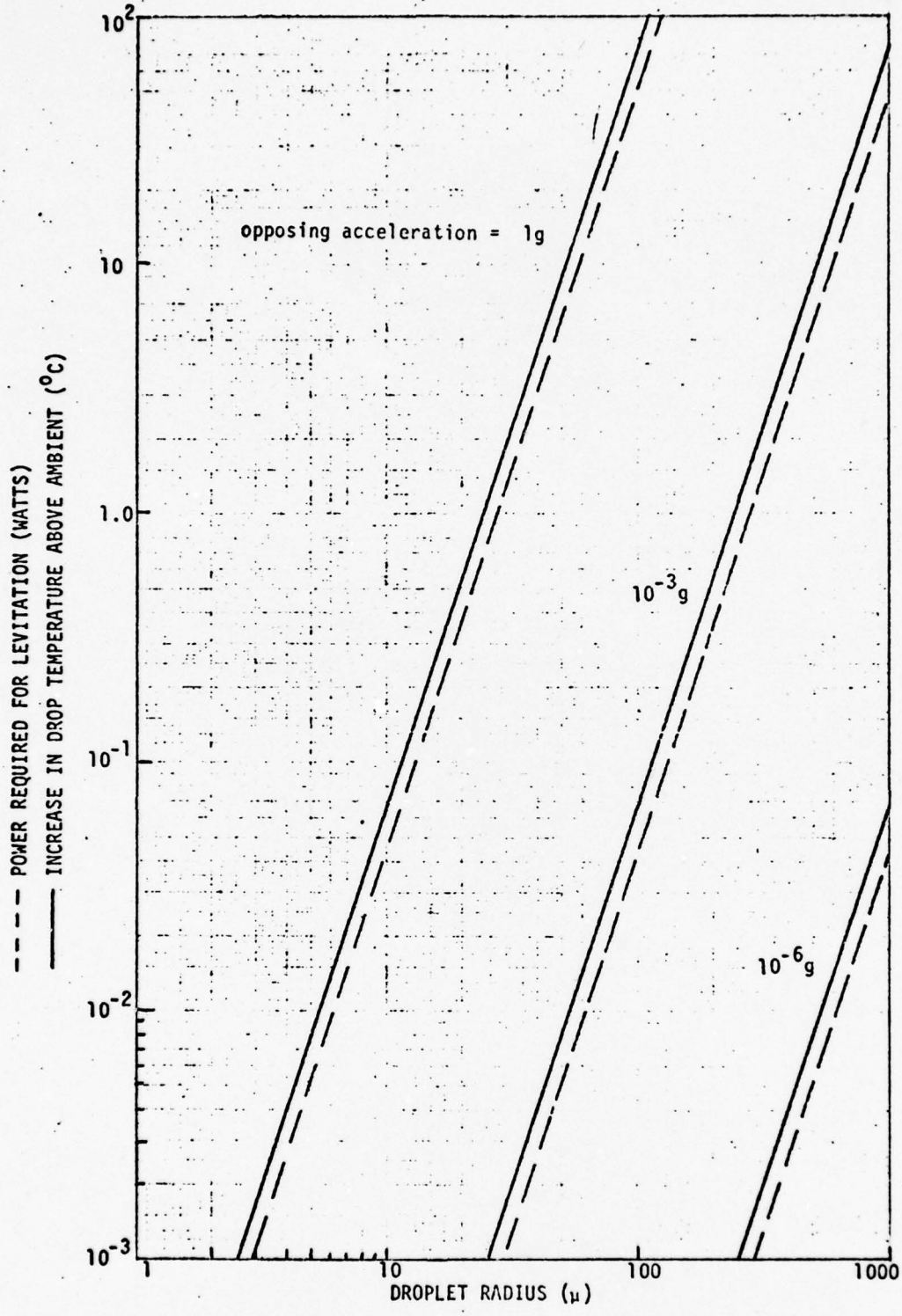

FIGURE 8. REQUIRED LEVITATION POWER AND CORRESPONDING TEMPERATURE RISE FOR A WATER DROPLET SUSPENDED IN AIR (T = 294°K, P = 1 ATM).

Substituting the values of $Q_{pr} = 0.26$ and $\rho = 1$ gm/cm^3, which are relevant to a water droplet, Equation (35) becomes:

$$a_{pr} = 2.07 \times 10^{-12} \text{ W/r}^3. \quad (36)$$

The variation of a_{pr} with changing values of r and W can now be easily calculated by alternately holding r and W at constant values. Figure 9 illustrates the variation of radiation pressure acceleration (a_{pr}) as a function of droplet radius for several values of laser power input. Similarly, Figure 10 indicates a_{pr} as a function of W for several values of r.

In order to obtain the net acceleration of the particle, the opposing acceleration (e.g., earth's gravity) must be subtracted from the values plotted in the figures. For example, working in a terrestrial laboratory with a 100 milliwatt laser, Figure 9 indicates that an acceleration of $\sim$ 1 g (980 cm/sec^2) can be given to a 14 μm radius droplet. However, this is just equal to the opposing acceleration of earth's gravity so that the net acceleration of the droplet is zero. If the same laser were used in the Spacelab where a typical acceleration level might be $\sim 10^{-3}$ g (Figure 1) the net acceleration of the particle would be almost 1 g. Similarly, Figures 9 and 10 can be used to determine the net acceleration on a water droplet for various values of droplet size, laser input power and opposing acceleration field.

2.3.2 Wavelength Dependence of Levitation Power

The particle acceleration achieved is primarily a function of the Mie size parameter, $x = 2\pi r/\lambda$, which relates the particle radius (r) and the wavelength (λ). Maximum acceleration is achieved with $x \simeq 1$ (Adler, et al., 1972) with smaller local maximum at multiples of this value. In the present case of optical levitation ($\lambda \simeq 6328$ Å) being considered herein, $x >> 1$ for particles greater than one micron. As a result, the value of $Q_{pr} = 0.26$ will remain virtually unaffected as λ is varied within the bounds of the visible spectrum, and the levitation power required will remain constant.

For completeness, the acceleration magnitudes achievable in a vacuum from a broad spectrum of electromagnetic radiation sources is presented in Table II (Adler, et al., 1972). In all cases the power density was assumed to be 1 watt/cm^2 and the particle density 1 gm/cm^3. As a comparison, acoustical motion control as

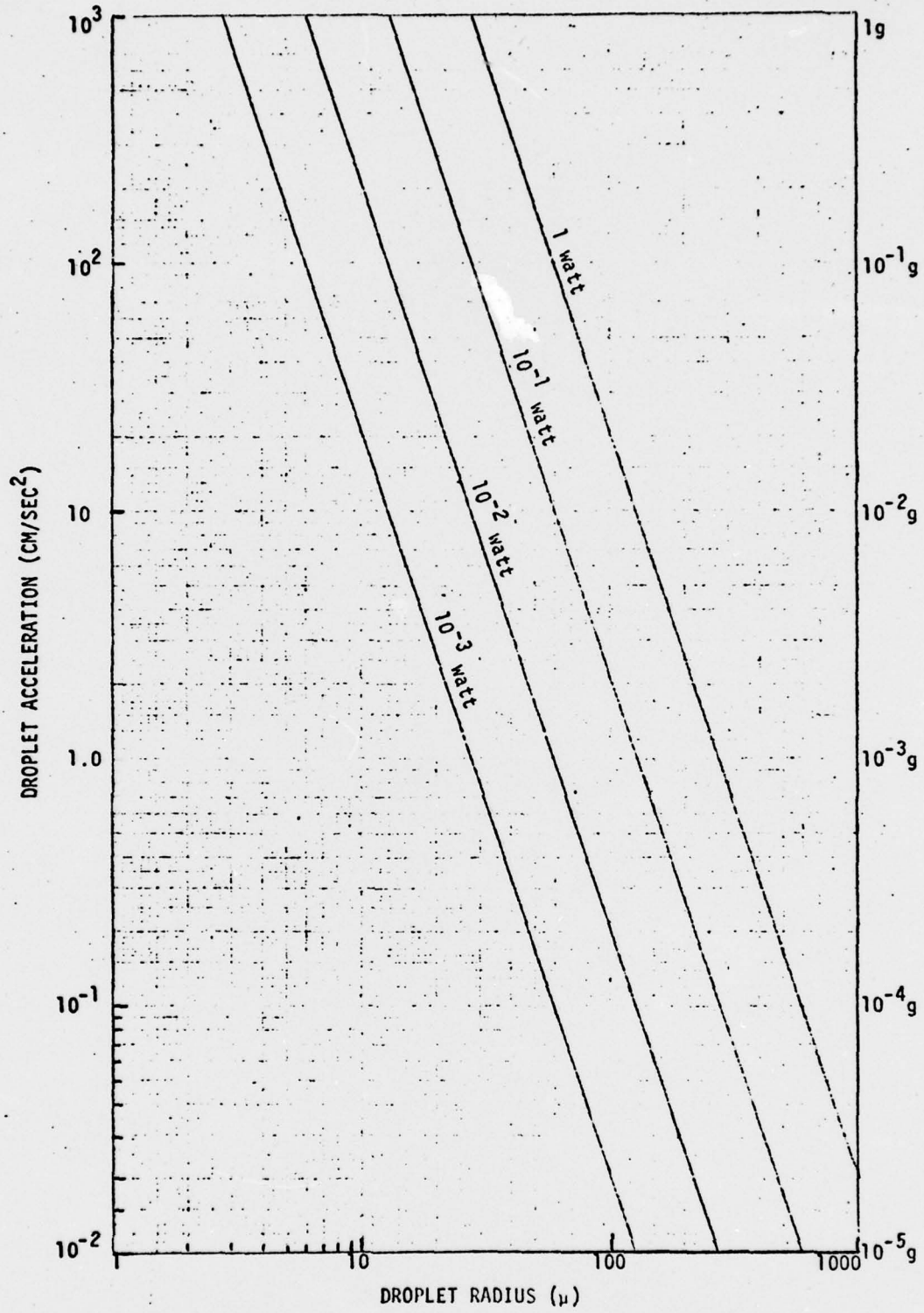

FIGURE 9. ACCELERATION DUE TO RADIATION PRESSURE AS A FUNCTION OF WATER DROPLET SIZE FOR SEVERAL LASER POWER LEVELS.

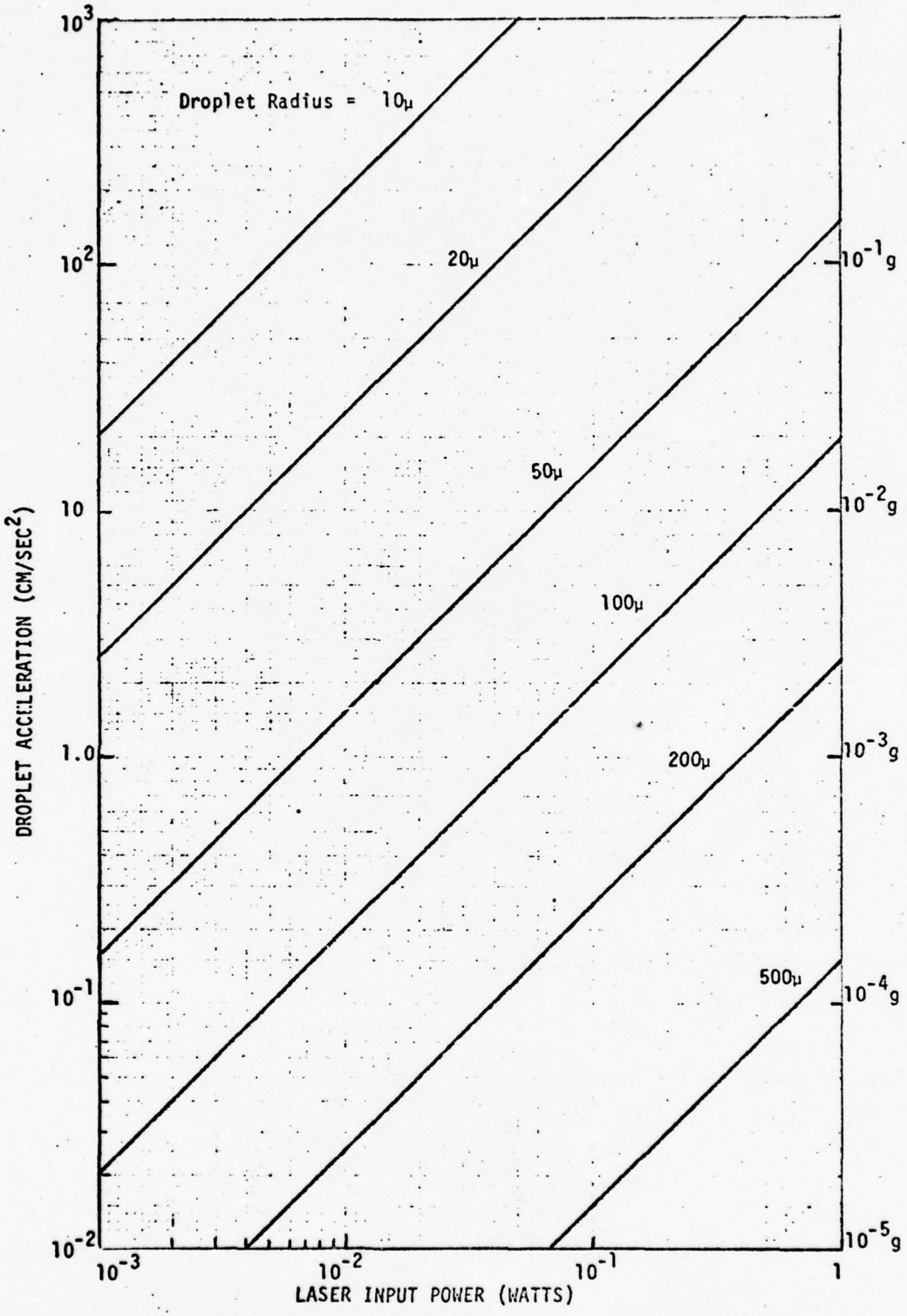

FIGURE 10. ACCELERATION DUE TO RADIATION PRESSURE AS A FUNCTION OF LASER POWER FOR SEVERAL WATER DROPLET SIZES.

TABLE II. ACCELERATION MAGNITUDES AS A FUNCTION OF WAVELENGTH OF INCIDENT ENERGY

Type of Radiation	Frequency Range	Nominal Wavelength	Min. Particle Diameter for Good Q_{pr}	Acceleration of the Minimum Particle
Microwave, X Band	8 - 12.5 GHz	3 cm	0.75 cm	0.00067 cm/sec^2
Microwave, K Band	18 - 26.5 GHZ	1 cm	0.25 cm	0.002 cm/sec^2
Microwave, O Band	60 - 120 GHz	0.3 cm	0.075 cm	0.0067 cm/sec^2
Infrared*, Submillimeter	1.2 x 10^{11} Hz - 10^{13} Hz	2500μ - 30μ	630μ - 7.5μ	.0079 cm/sec^2 - .67 cm/sec^2
Infrared, CO_2 Laser	2.83 x 10^{13} Hz	10.6μ	2.6μ	1.9 cm/sec^2
Visible Light	6 x 10^{14} Hz	0.5μ	0.12μ	40 cm/sec^2
Ultra Violet	6 x 10^{15} Hz	0.05μ	0.012μ	400 cm/sec^2
X-Rays* and γ Rays	10^{17} - 10^{22} Hz	30A - 0.0003Å	1.0Å (atoms)	0.0026 cm/sec^2

*Note that the power density in these regions which is currently available from state-of-the-art power sources is generally much less than 1 watt/cm^2 so that in practical equipment the accelerations achievable in the asterisked rows would be proportionally less than the values shown. X-ray power is about 10^{-2} watts/cm^2, and except for a few experimental lasers at a few hundred microns, there aren't any good sources in the submillimeter region.

being developed by Jet Propulsion Laboratory has effective wavelengths of greater tha 3 cm and therefore is restricted to particle radii greater than a centimeter. From this table, infrared and visible electromagnetic radiation are the most suitable for motion control of the micrometer radii of interest in atmospheric precipitation processes involving the growth transition zone between pure diffusional growth and the dynamic collision/coalescence growth.

Thus, along with the ability to operate at a distance, manipulate selected particles in a group of particles and minimal effects on the particle physical characteristics, the visible and near visible radiation exerts the optimum forces on the particles of interest as well as being available at the power densities (lasers) required to be implemented.

2.3.3 Typical Velocity Levels

A water drop being accelerated in air by a constant applied force will eventually attain an equilibrium velocity (v) determined by the resistive drag force which can be expressed as follows (Mason, 1971):

$$F_d = \frac{\pi r^2}{2} C_d \rho_g v^2 \tag{37}$$

where C_d is the drag coefficient and is a function of the Reynolds number R_e,

$$R_e = \frac{2 v r \rho_g}{\eta} \tag{38}$$

defined by the equation:

$$\frac{C_d R_e}{24} = \frac{F_d}{6 \pi \eta r v} \tag{39}$$

The drag force can then be expressed as

$$F_d = \left(\frac{C_d R_e}{24}\right) 6 \pi \eta r v \tag{40}$$

and the force equation for the drop becomes:

$$m\left(\frac{dv}{dt}\right) = ma - \left(\frac{C_d\ R_e}{24}\right) 6\ \pi\ \eta\ r\ v \tag{41}$$

The left side of Equation (41) is just the net force acting on the droplet. The first term on the right is the accelerating force acting on the droplet (neglecting the buoyancy of air), while the second term in the previously defined drag force, at equilibrium (i.e., dv/dt = 0). Equation (41) can be solved for the velocity to obtain:

$$v = \left(\frac{24}{C_d\ R_e}\right)\ \frac{ma}{6\ \pi\ \eta\ r} \tag{42}$$

Substituting for the particle mass we have:

$$v = \left(\frac{24}{C_d\ R_e}\right)\ \frac{2}{9}\ \frac{\rho r^2}{\eta}\ a. \tag{43}$$

In the case of Stokes Law ($R_e \leq 0.1$), $C_d\ R_e = 24$ and Equation (39) becomes:

$$v = \frac{2}{9}\ \rho \frac{r^2 a}{\eta}. \tag{44}$$

As R_e becomes larger, Stokes Law increasingly overestimates the actual velocity so that empirical relations between $C_d\ R_e$ and R_e are usually used. The data of Beard and Pruppacher (1969) showed that water drops can be well represented by the following formulae given by Mason (1971):

$$\frac{C_d\ R_e}{24} = 1 + 0.10\ R_e^{0.955},\ 0.01 \leq R_e \leq 2, \tag{45a}$$

$$= 1 + 0.11\ R_e^{0.81},\ 2 \leq R_e \leq 21, \tag{45b}$$

$$= 1 + 0.189\ R_e^{0.632},\ 21 \leq R_e \leq 200$$

In practice $C_d\ R_e^2$ is usually plotted as a function of R_e as shown in Figure 11. The quantity of $C_d\ R_e^2$ can be expressed in terms of the drop radius, the air (ambient) characteristics and the acceleration level as (Beard and Pruppacher, 1969):

$$C_d\ R_e^2 = \frac{32}{3}\ r^3\ \rho_g\ \rho\ \frac{a}{\eta^2} \tag{46}$$

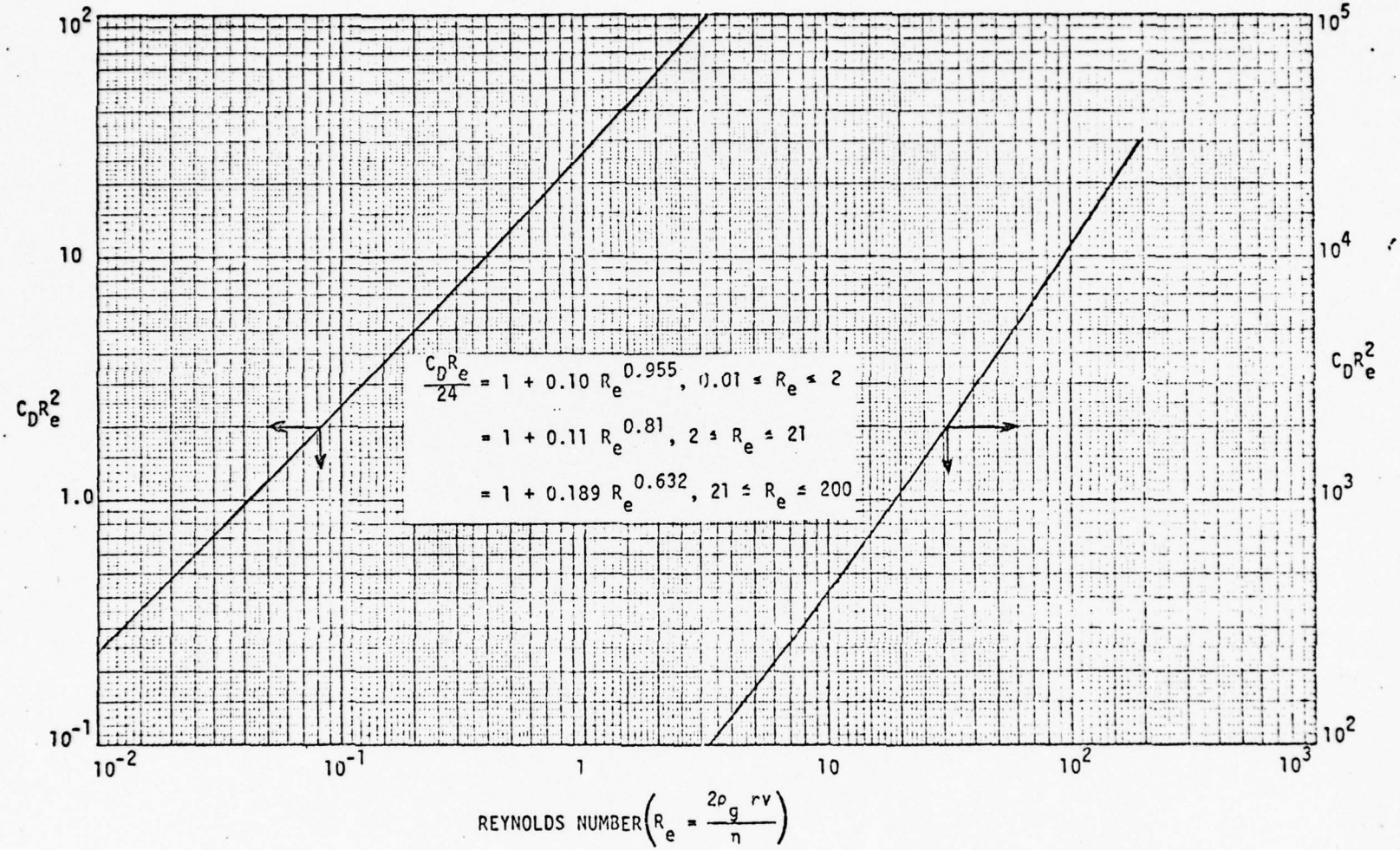

FIGURE 11. $C_DR_e^2$ AS A FUNCTION OF REYNOLDS NUMBER
(FROM MASON, 1971)

where a is the net acceleration of the particle. Thus the procedure for calculating the equilibrium velocity of a water droplet is as follows:

1. Specify the drop characteristics (r,ρ), the ambient characteristics (ρ_g,η), and the net acceleration (a).
2. Calculate $C_d R_e^2$ from Equation (46).
3. Determine the corresponding value of R_e from Figure 11.
4. If $R_e < 0.1$ calculate v from Equation (44).
5. If $R_e \geq 0.1$ calculate v from Equation (45).

Figure 12 illustrates the equilibrium or terminal velocity attained by a water droplet in air (T = 294 °K, P = 1 atm) for various multiples of earth's gravity (g).

In order to utilize laser energy to control the motion and position of a droplet, the acceleration imparted to it must be sufficient to exceed the opposing acceleration field (e.g., earth's gravity in a terrestrial laboratory). In Figures 13, 14, and 15 the equilibrium velocity has been plotted as a function of droplet radius for various values of laser input power. The three figures illustrate the limitations imposed by three different opposing acceleration fields, i.e., 1 g, 10^{-3} g, and 10^{-6} g, respectively. The second and third acceleration levels are typical of what may be called the random and known values, respectively (refer to Figure 1). The surrounding medium is again assumed to be air at T = 294 °K and P = 1 atm.

In each figure the equilibrium velocities which would pertain if there were no opposing acceleration are indicated by the dashed lines. Also shown on these figures is the terminal velocity a droplet would have in the earth's atmosphere for the conditions of 1 g, T = 294 °K and P = 1 atm. Thus, if it is desired to simulate droplet collisions resembling those which might be naturally occuring in the atmosphere, the "1 g" dot-dash line shown in the figures can be used as a guide in determining the laser power required for a given drop size. If a particular experiment requires precise positioning of a droplet, the droplet velocity must be relatively low, e.g., < 0.1 cm/sec. The optimum laser power to achieve this goal can be obtained by referring to the proper figure.

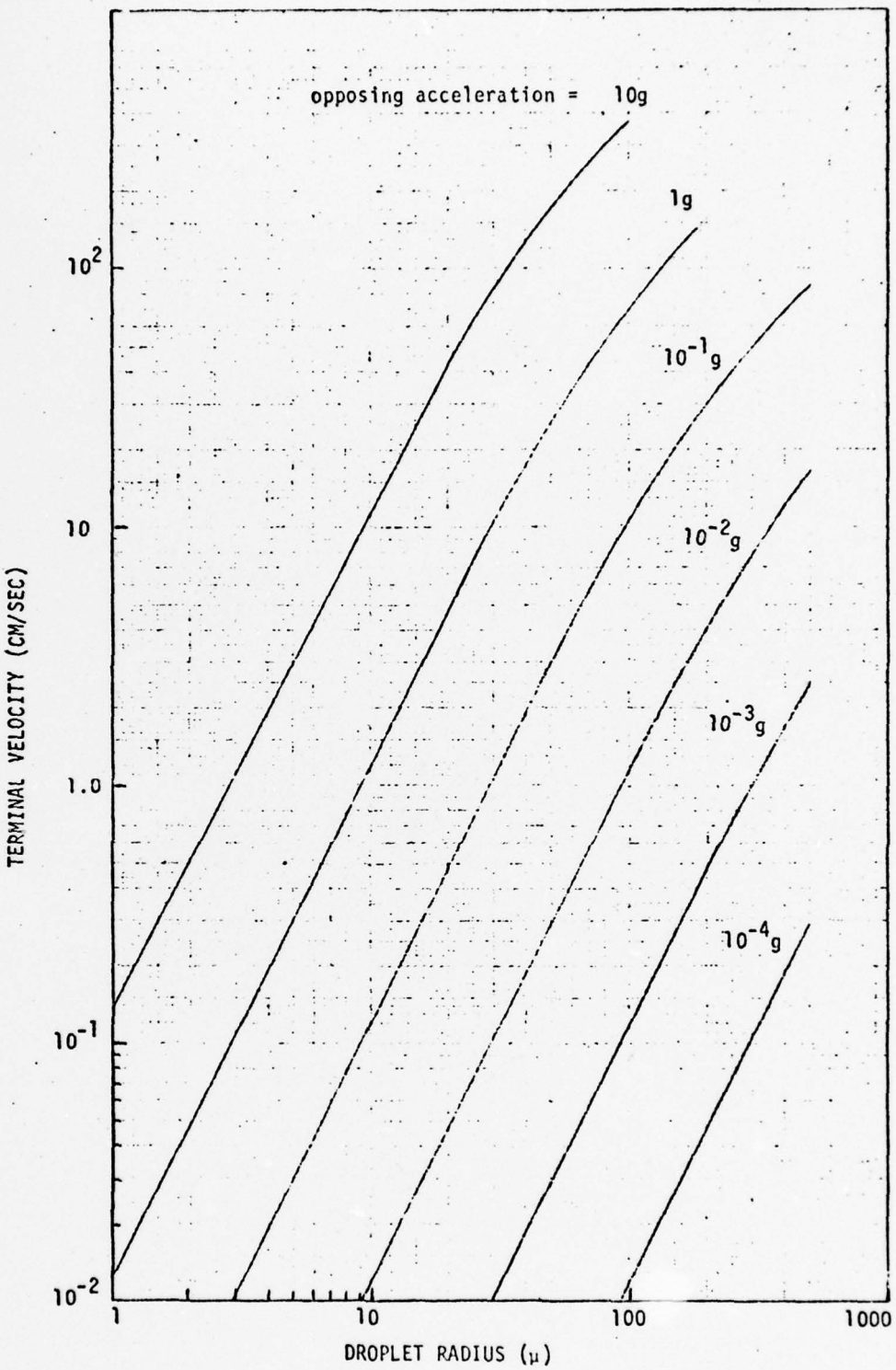

FIGURE 12. WATER DROPLET VELOCITY IN AIR (T = 294°K, P = 1 ATM) FOR SEVERAL VALUES OF OPPOSING ACCELERATION (g = 980 CM/SEC^2).

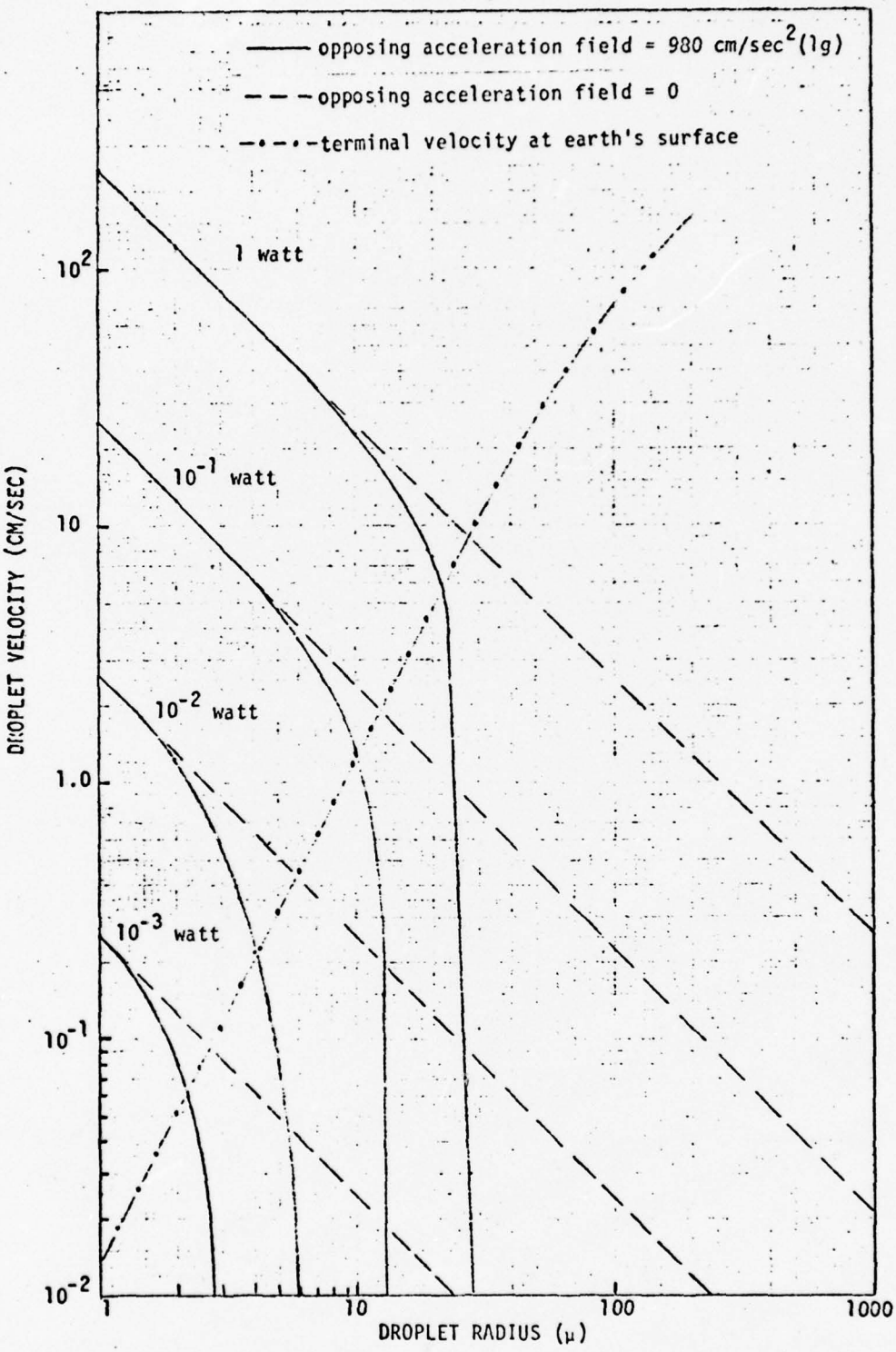

FIGURE 13. WATER DROPLET VELOCITY AS A FUNCTION OF DROPLET SIZE (OPPOSING ACCELERATION = 1g).

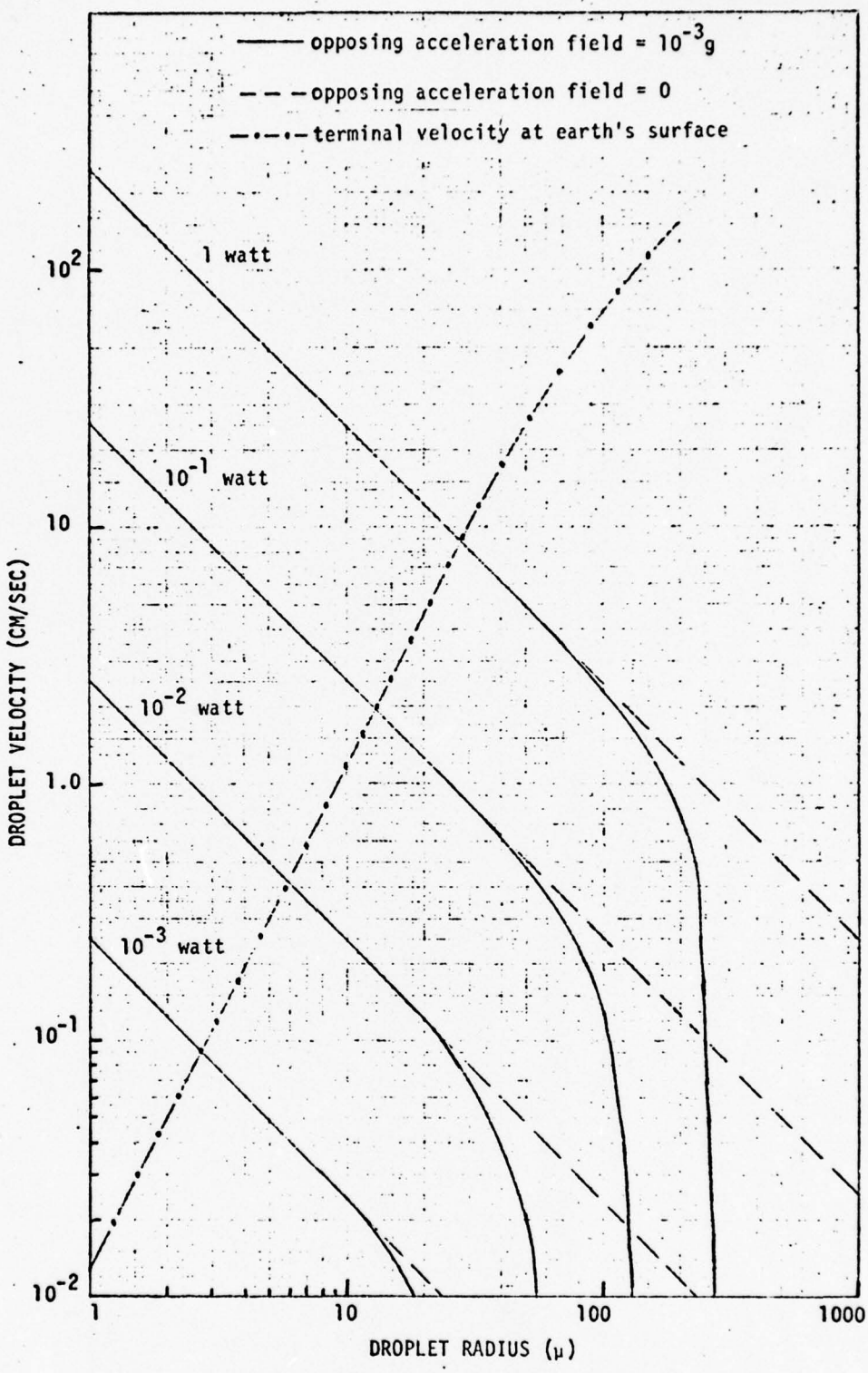

FIGURE 14. WATER DROPLET VELOCITY AS A FUNCTION OF DROPLET SIZE (OPPOSING ACCELERATION = 10^{-3}g).

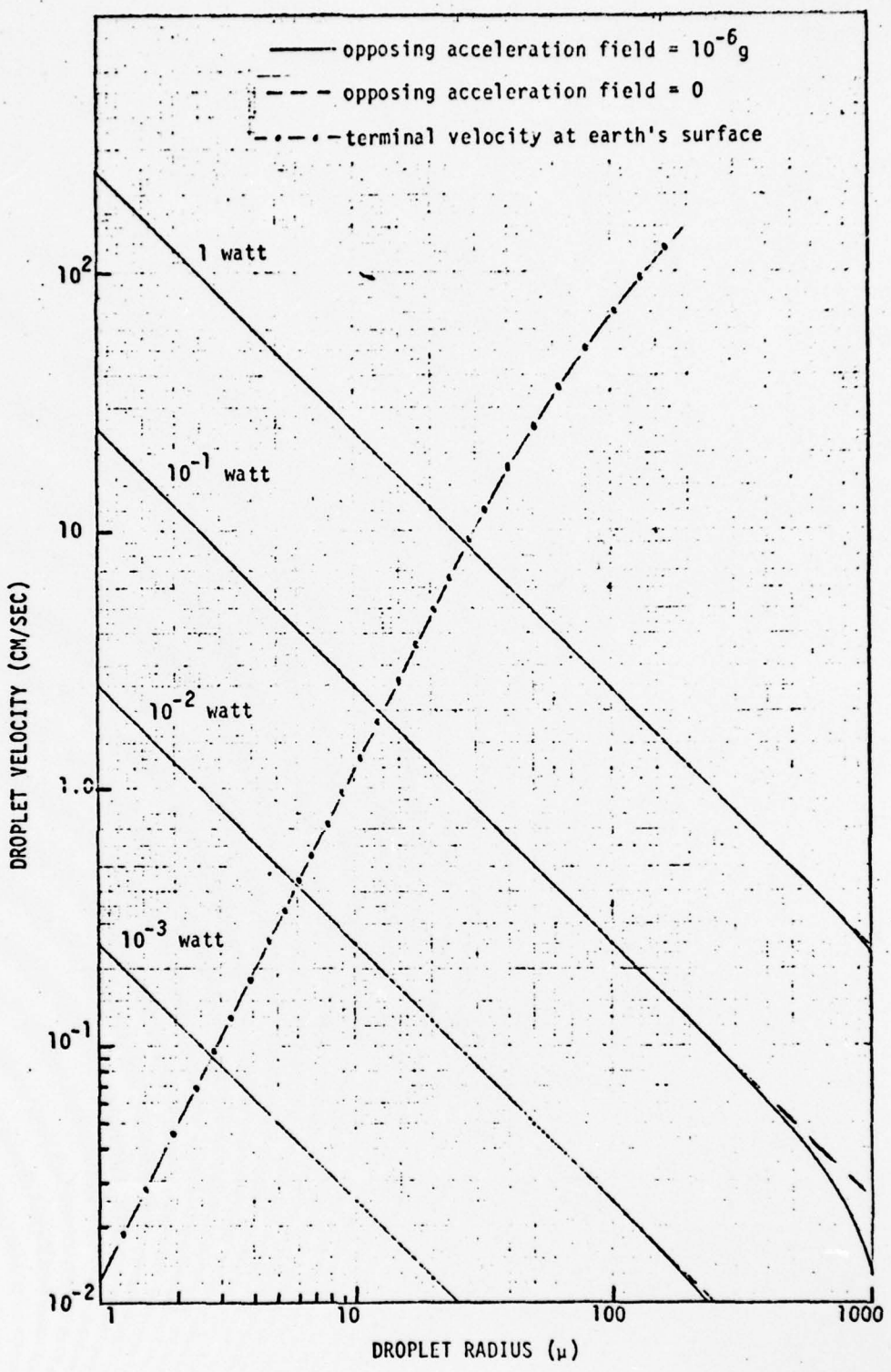

FIGURE 15. WATER DROPLET VELOCITY AS A FUNCTION OF DROPLET SIZE (OPPOSING ACCELERATION = 10^{-6}g).

Similar results are presented in Figures 16, 17, and 18. However, in this case the independent variable is the laser input power and the equilibrium velocity is presented for a range of droplet sizes. These figures can be used by themselves, or in combination with the three previously discussed figures to define the laser input power appropriate for a given experiment. The obvious point illustrated by these figures is however the increased versatility and applicability of optical motion control as one moves from a terrestrial laboratory to Spacelab.

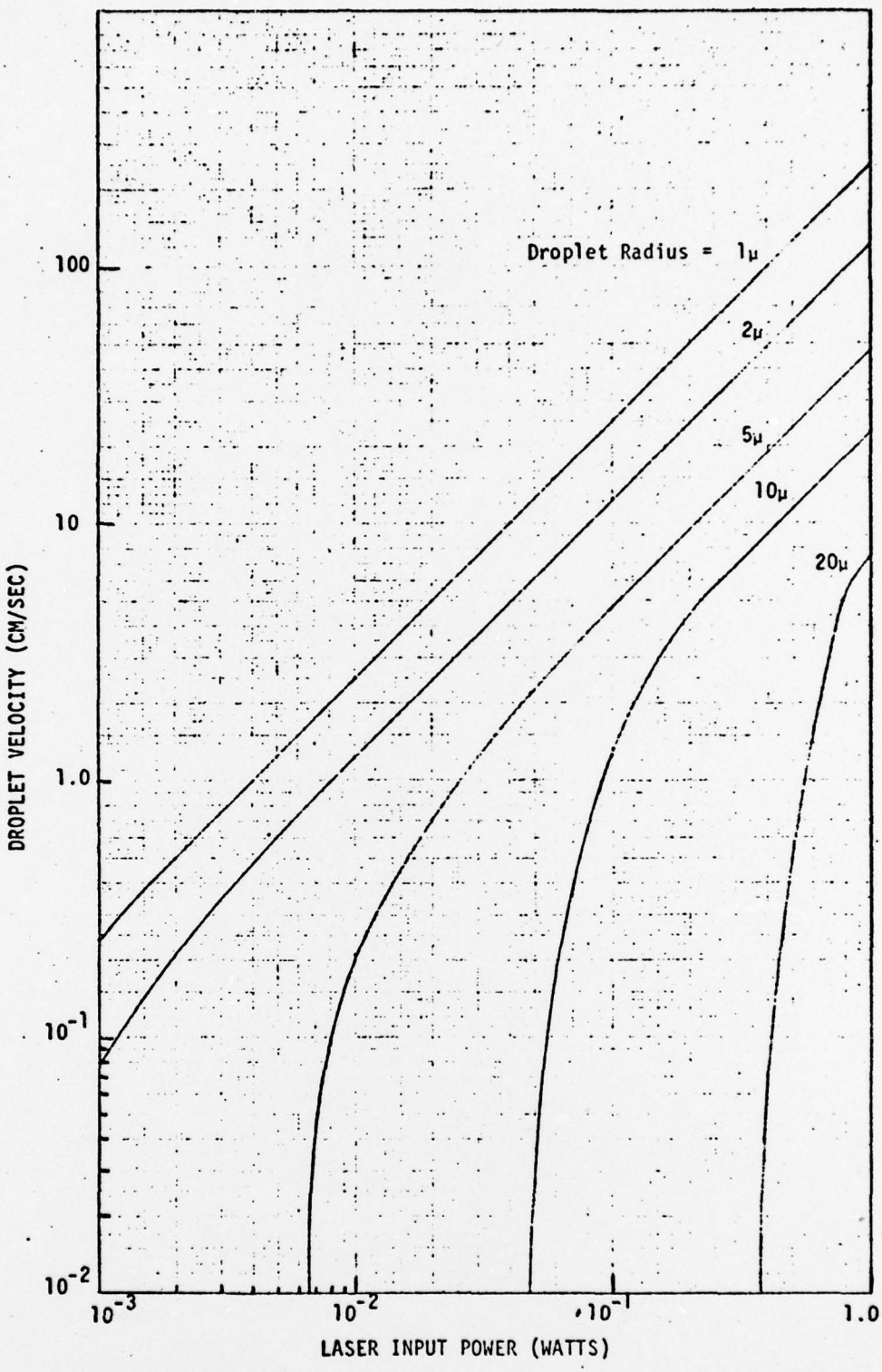

FIGURE 16. WATER DROPLET VELOCITY AS A FUNCTION OF LASER POWER (OPPOSING ACCELERATION = 1g).

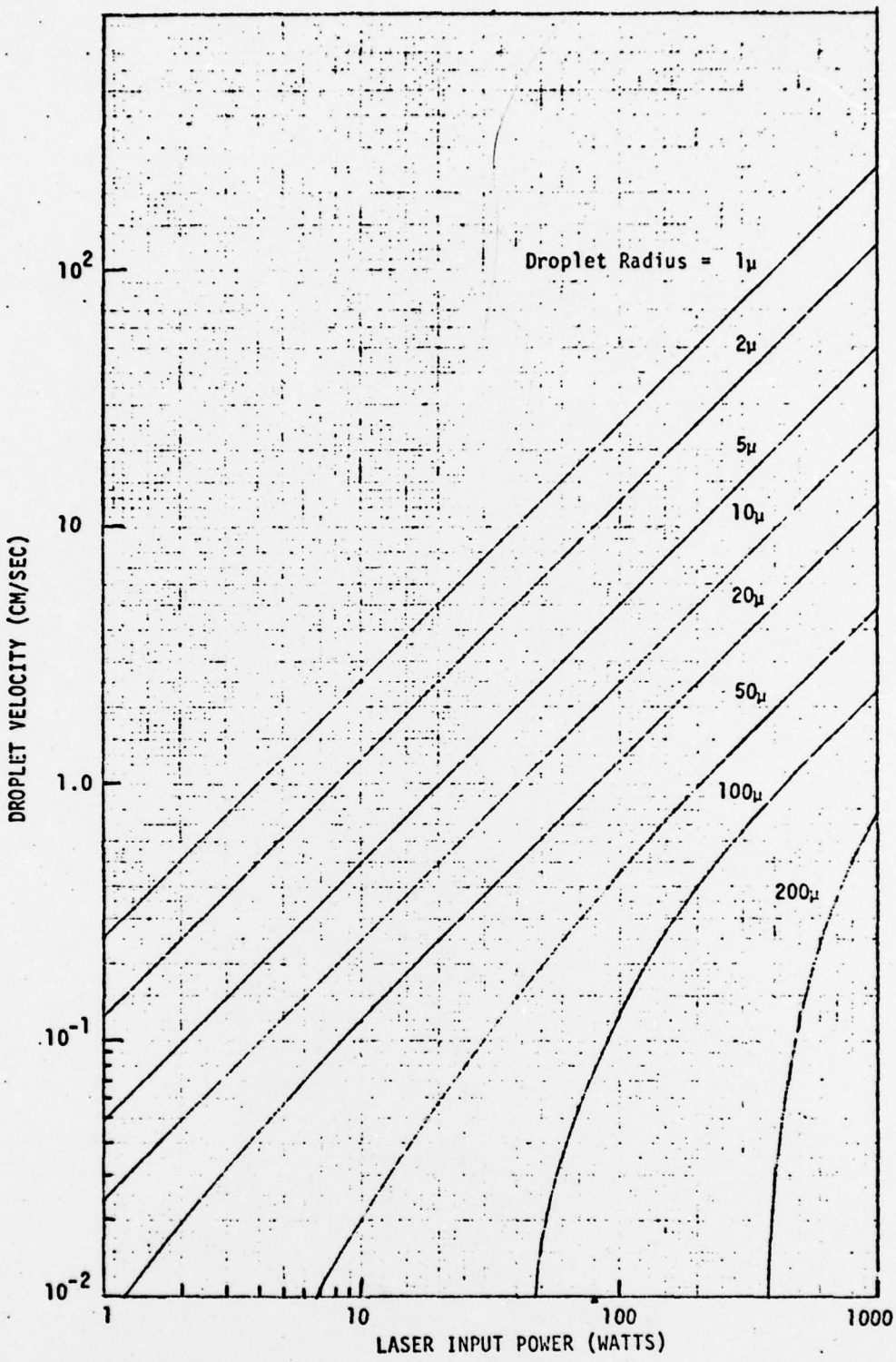

FIGURE 17. WATER DROPLET VELOCITY AS A FUNCTION OF LASER POWER (OPPOSING ACCELERATION = 10^{-3}g).

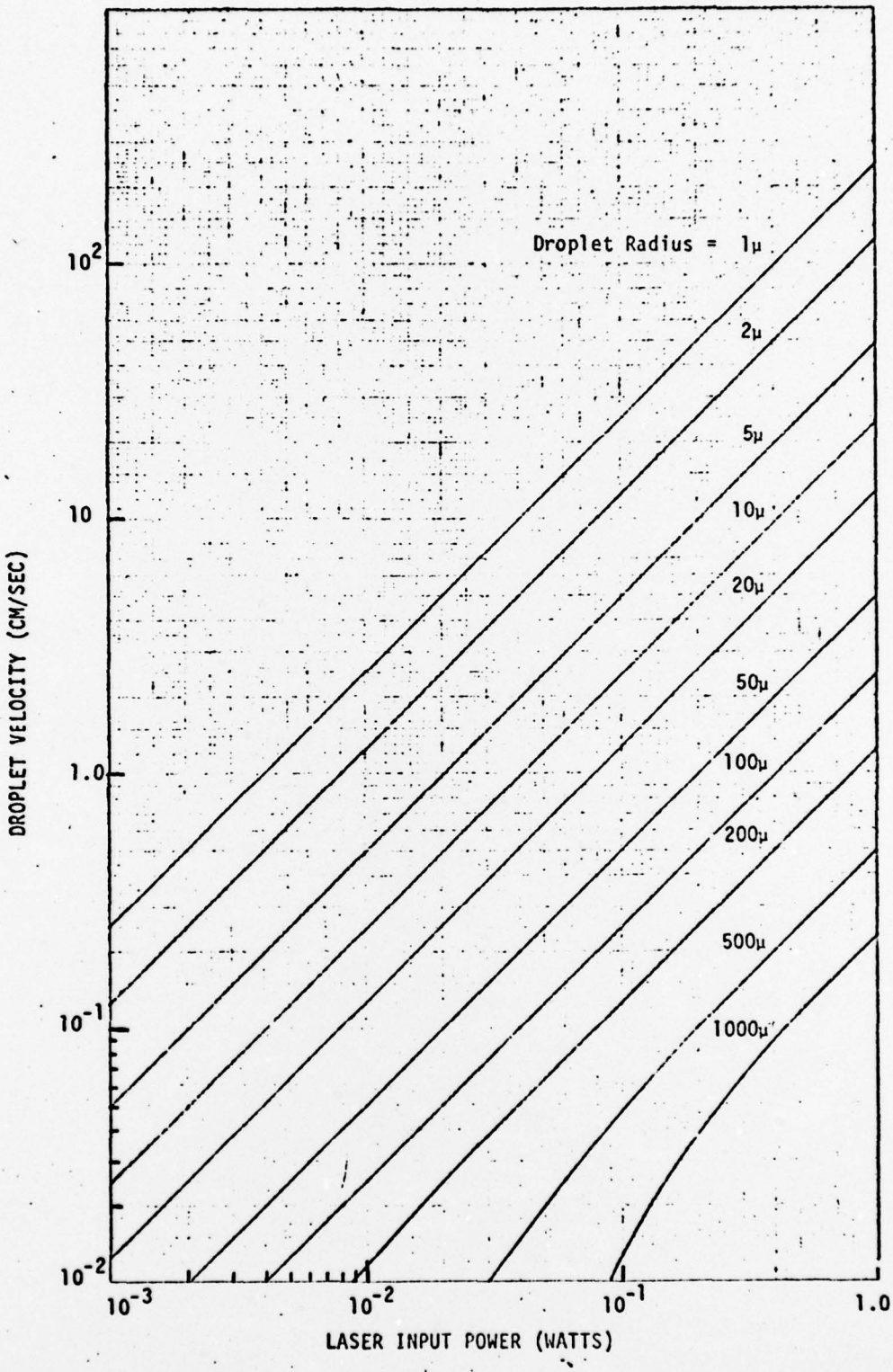

FIGURE 18. WATER DROPLET VELOCITY AS A FUNCTION OF LASER POWER (OPPOSING ACCELERATION = 10^{-6}g).

3.0 APPLICABILITY OF OPTICAL MOTION CONTROL TO CLOUD PHYSICS STUDIES

3.1 Atmospheric Cloud Physics Laboratory on Shuttle/Spacelab.

The previous sections have shown that the utilization of optical motion control (OMC) is primarily determined by the available laser power. The Air Force (among others) is currently developing a space qualified laser (Program 405B) for use in satellite-to-satellite communications which will be compatible for use on Shuttle/Spacelab. This laser will operate at a wavelength of 0.532 μm with a power output of between 100 to 200 mW and will be available around 1979. We can, therefore, assume that the first application of OMC to the ACPL will have a useable laser power of 100 mW. In addition, we can assume that the maximum residual or ambient acceleration in the Spacelab is 10^{-3} g (cf. Figure 1). Within these bounds we can define the applicability of OMC for experiments relating to: (1) the growth of water droplets or ice crystals, and (2) the collision or coalesence of two or more drops or crystals.

The role of OMC in the first of these applications will depend on the method by which the droplets or crystals are generated. For example, they may be generated "in position" within the supersaturated environment of a static diffusion chamber. The laser beam would then be used as a probe to select and hold an individual droplet in position so that its growth history could be observed. An alternate method would be to generate droplets singly (e.g., using a wire probe retractor) near the edge of the chamber and then use the laser energy to move the droplet into a location where it could be fixed in a viewing position by a second laser beam. The droplet size range to which these applications can be applied can be easily visualized by referring to Figure 19 (this is a modified version of Figure 14, Section 2.3.3).

Droplet sizes in the range of 5-100 μm radius are of particular interest for cloud physics investigations on the microphysical level. The cross-hatched area in Figure 19 indicates the maximum velocities which can be expected for an applied laser power of 100 mW. Droplets with radii less than $\sim$ 13 μm can be accelerated to velocities which are greater than their respective terminal earth's atmosphere (1 g) velocities. Dynamic processes such as scavenging, and collision/coalescence can therefore be simulated and observed in zero g as they might naturally occur in the 1 g earth environment but with better control and longer observation times. Figure 19 also illustrates that the upper size limit for position control

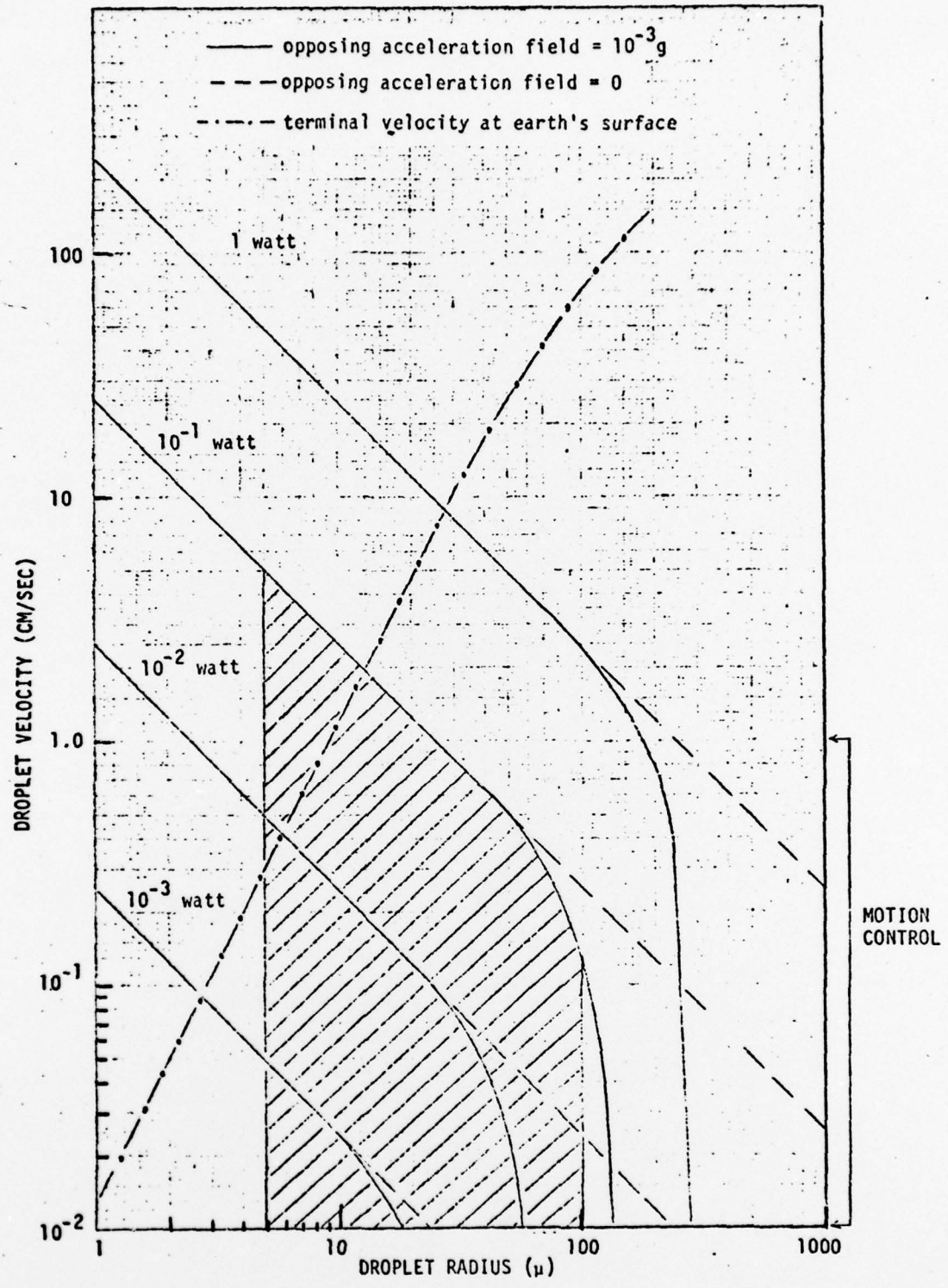

FIGURE 19. WATER DROPLET VELOCITY AS A FUNCTION OF DROPLET SIZE. CROSS-HATCHED AREA INDICATES REGION OF APPLICABILITY FOR SHUTTLE/SPACELAB EXPERIMENTS (ASSUMING 100 mW LASER).

of water droplets will occur at $\sim$ 130 μm (the size for which the 100 mW curve becomes essentially vertical). This size limit could also be obtained from Figure 9 by noting the droplet size at which its radiation pressure acceleration is equal to the opposing ambient acceleration of 10^{-3} g.

Thus OMC can provide a significant contribution to atmospheric microphysics experimentation in ACPL through positioning and variable accelerated motion control.

3.2 Terrestrial Laboratory

In principle, the utilization of OMC to perform cloud physics experiments in a terrestrial laboratory is not limited by the available laser power. However, as was shown in Figure 8, the droplet temperature increases rapidly as the laser input power is increased. Thus, the applicability of OMC will be determined by the acceptable temperature rise of the droplet. For example, if the maximum tolerable droplet temperature increase were 10 °C then the maximum droplet size cutoff would occur at $\sim$ 50 μm radius (laser power imput of $\sim$ 700 mW), which is well below the previously discussed limit of $\sim$ 130 μm for the ACPL on Shuttle. Note that from Figure 8 the power required to levitate a 100 μm water droplet would also raise its temperature to the boiling point (1 g conditions).

On the basis of the above considerations terrestrial applications of OMC to water droplets will be confined to radii less than $\sim$ 50 μm. However, earth based laboratory experiments with OMC will be necessary to provide proper development of motion and position control techniques which may subsequently be implemented on the Shuttle/Spacelab ACPL.

4.0 OPTICAL MOTION CONTROL CONCEPT FOR ACPL

A summary of potential ACPL experiments which would benefit from the implementation of optical motion control capability is presented in Table III. A potential experiment illustrating a specific application of OMC is outlined below.

Assume that the experiment objective is to monitor the growth history of an individual water dropler (or ice crystal) for an extended period of time. A typical protocol would be as follows:

1. A 25 μm radius water droplet is generated at the outer edge of a chamber (e.g., static diffusion chamber) which has a radius of 15 cm.
2. A 100 mW laser is then used to move the droplet to the center of the chamber, a distance of 15 cm, in approximately 15 sec (from Figure 19).
3. The droplet is then held in this position by an additional laser beam of equal power so that its growth history can be monitored. (Note: the diffraction pattern from the droplet can be used for a precise measurement of its size.)
4. The droplet will continue to grow until its radius is approximately 130 μm. As it approaches and exceeds this size, ambient acceleration forces will eventually dominate the applied radiation pressure forces and the droplet will be lost.

A sketch illustrating the experiment configuration is given in Figure 20.

Similar scenarios can be envisioned for droplet collision/coalescence experiments where impact parameters can be predetermined to better than one micrometer. The droplets can be accelerated toward each other or in the same direction with velocities representative of 1g, 0.1 g, etc. acceleration fields. The repeatable and precise control will permit a better assessment of the effects of charge, surfactants, etc. on droplet/droplet and droplet/ice interactions.

TABLE III. ACPL EXPERIMENT MOTION CONTROL REQUIREMENTS

Experiment Class		Applicable Aspects	REQUIREMENT Alignment	Velocity
Class 3	Ice Multiplication	e.g., collision of ice/ice or ice/water		x
Class 4	Charge Separation	e.g., collision of ice/ice or ice/water in presence of d.c. electric field	x	x
Class 5	Ice Crystal Growth Habits	To offset the 10^{-3} to 10^{-5} g drift for extended observation periods and to align crystal for optimum photography	x	
Class 6	Scavenging	*Dynamic scavenging processes - motion of* large ice/water particles through field of smaller particles		x
Class 7	Riming and Aggregation	Dynamic interaction between ice/ice and ice/water requires precise motion control	x	x
Class 10	Collision-Induced Freezing	Motion control to initiate the collision		x
Class 11	Supercooled - Water Saturation Vapor Pressure	Provide the extended time required for equilibrium	x	
Class 17	Droplet Collision	Motion control to provide relative velocities		x
Class 18	Coalescence Efficiencies	Precise control of particle motion to provide known low-acceleration, relative motion between particles		x
Class 20	Unventilated Droplet Diffusion Coefficient	Position control for extended observation periods	x	

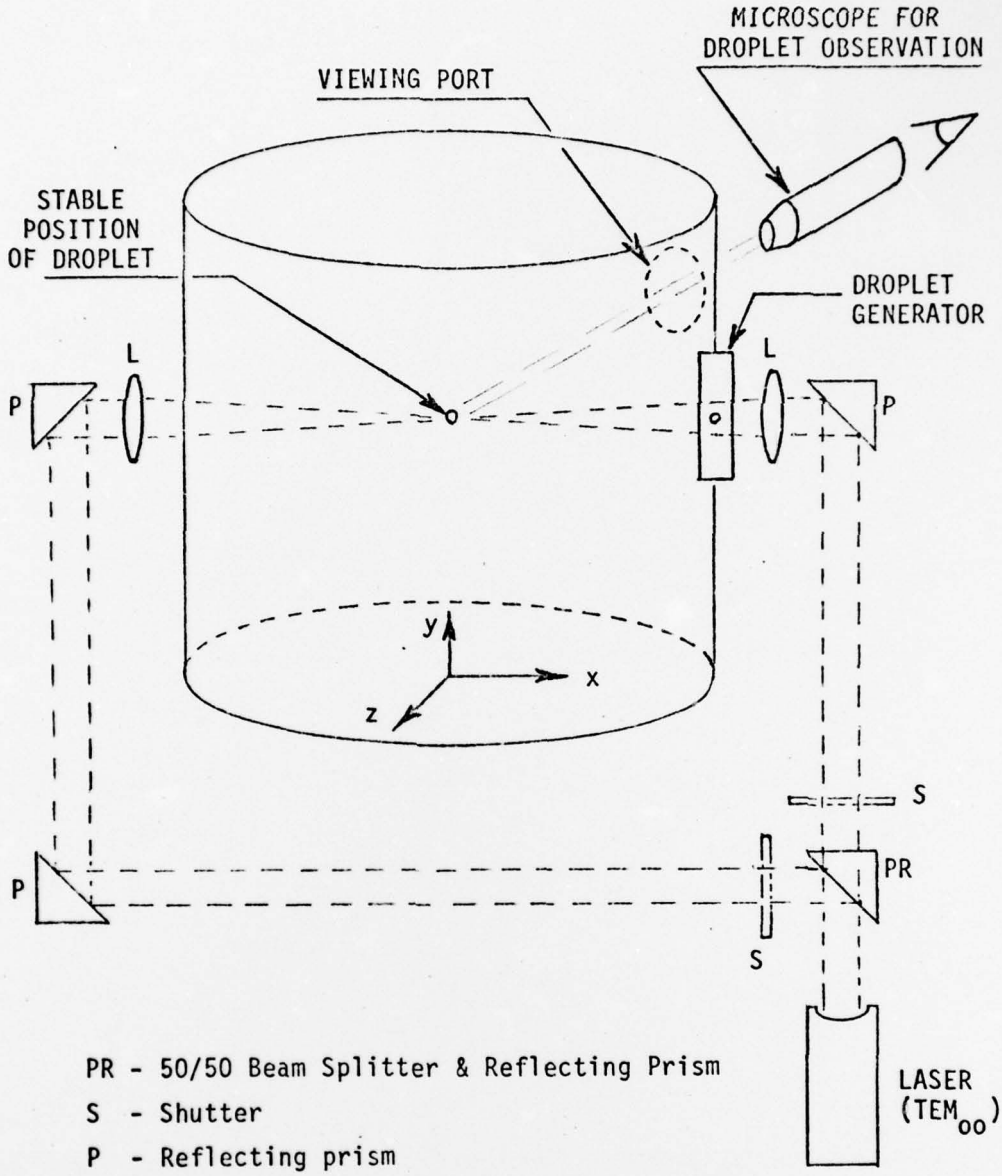

- Stability in x direction provided by opposing laser beams
- Stability in y and z direction provided by transverse restoring force of gaussian beam

FIGURE 20. ILLUSTRATION OF THE EXPERIMENT CONFIGURATION FOR GENERATING AND POSITIONING A WATER DROPLET TO DETERMINE ITS GROWTH HISTORY.

5.0 PROGRAM FOR FUTURE WORK

This study indicates that continued investigation (primarily in the laboratory) of the potential application of OMC to atmospheric cloud physics problems will provide valuable insight into several microphysical phenomena. For example, experimental determination of the coalescence efficiencies of cloud droplets in the growth transition region between 8 and 15 μm radius has been severely hampered due to the lack of sufficiently accurate control of these small droplets. As discussed in the previous section these sizes are well within the range for which OMC is applicable to a terrestrial laboratory. In addition, Dr. Ashkin of the Bell Telephone Laboratories has demonstrated the precise positioning capability (positioning accuracies of a few micrometers) of OMC in his laboratory. The use of optical levitation will permit the establishment of accurate initial relative positions between two drops which, upon release, will undergo a collision/coalescence process. The benefits of this technique are further enhanced when it is used in conjunction with a drop generator (such as a wire probe retractor) which can repeatedly generate individual drops with a given size and trajectory (i.e., fall velocity). It will then be possible to precisely control the impact parameter permitting the investigation of various droplet interactions as the impact parameter is varied. Thus, the influence of droplet charge, electric fields, surfactants and turbulence on the collision/coalescence process in the size range between 8 and 15 μm radius can be studied. The investigations will also provide a means of evaluating the utility of optical motion control for experiments in the ACPL. In addition, this levitation technique may be extended to the study of ice crystal electrification and coagulation (sticking coefficient determination).

The basic equipment to implement these concepts currently exists in the General Electric Space Sciences Laboratory. In particular the following items are available:

1. 50 mW Helium-Neon laser.
2. 2.5 W Argon laser.
3. Aerosol generators and atomizers for producing a cloud of droplets.
4. Wire probe retractor and vibrating orfice generators for generating individual drops.
5. Microscopes for observing droplet interactions.

A program for laboratory evaluation of the OMC concept as applied to atmospheric cloud physics is given below.

Experimental Objectives

1. Generate a cloud of droplets and demonstrate the capability of capturing and levitating individual droplets composed of a non-volatile substance such as silicon oil.

2. Repeat objective 1 using water droplets. This objective will require the design of a container to provide a saturated environment for the droplet to prevent evaporation.

3. Implement the wire probe reactor to operate in conjunction with the optical levitation technique (i.e., generate and capture individual drops with repeatability).

4. Utilize the wire probe retractor to generate drops which fall past another drop held in position by the laser beam. The effect of varying drop size and impact parameter can be studied.

5. Utilize the procedure of objective 4 to investigate the influence of droplet charge, electric fields, surfactants and turbulence on the collision/coalescence process.

6. Implement a technique recently developed by Ashkin and Dziedzic (personal communication, 1977) to provide feedback stabilization of optically levitated particles.

It should be noted that the above program objectives are structured in a manner which permits them to be accomplished incrementally, i.e., each objective contributes to those which follow. The exception is objective 6 which is relatively independent of the others. This technique is most important when working at low pressures where the viscous damping forces become small and for extended operation in zero g where the laser power is turned up periodically for repositioning as needed and turned to a low level standby to provide position sensing. In conclusion, useful scientific information is provided by each of the first five objectives while also contributing toward evaluating the OMC concept for use in the ACPL on Shuttle/Spacelab.

6.0 REFERENCES AND BIBLIOGRAPHY

6.1 References

Adler, M.S., Savkar, S. D., and Summerhayer, H. R., "Manipulation of Particles by Weak Forces in Zero G Environment", A report for Space Systems Department of General Electric by Physics & Electrical Engineering Laboratory, Corporate Research & Development, General Electric Co., Schenectady, N.Y., July 1972.

Ashkin, A., "Acceleration and Trapping of Particles by Radiation Pressure", Physical Review Letters, Vol. 24, No. 4, pp. 156-159, 26 January 1970.

Askin, A., and Dziedzic, J. M., "Optical Levitation by Radiation Pressure", Applied Physics Letters, Vol. 19, No. 8, pp. 283-285, 15 October 1971.

Ashkin, A., and Dziedzic, J. M., "Stability of Optical Levitation by Radiation Pressure", Applied Physics Letters, Vol. 24, No. 12, pp. 586-588, 15 June 1974.

Beard, K. V., and Pruppacher, H. R., "A Determination of the Terminal Velocity and Drag of Small Water Drops by Means of a Wind Tunnel", Journal of the Atmospheric Sciences, Vol. 26, No. 9, 1969.

Eaton, L. R., Cloud Droplet Interactions, Ph.D. Thesis, Department of Physics, University of Nevada, Reno, 1971.

Final Report - The Initial Atmospheric Cloud Physics Laboratory (ACPL) Spacelab Mission Payload, MA-05, Vol. 1, Prepared for NASA-Marshall Space Flight Center by General Electric Space Division, January 1977.

Fuchs, N. A., The Mechanics of Aerosols, The Macmillan Company, New York, 1964

Mason, B. J., The Physics of Clouds, Clarendon Press, Oxford, 1971.

Schwehm, G., Personal Communication (1976).

van de Hulst, H. C., Light Scattering by Small Particles, John Wiley & Sons, Inc., New York, 1957.

6.2 Bibliography

Ashkin, A., and Dziedzic, "Optical Levitation of Liquid Drops by Radiation Pressure", Science, Vol. 187, pp. 1073-1075, 21 March 1975.

Ashkin, A., and Dziedzic, J. M., "Observation of a New Nonlinear Photoelectric Effect Using Optical Levitation", Physical Review Letters, Vol. 36, 267, 1976.

Ashkin, A., Dziedzic, J. M., "Radiation Pressure on a Free Liquid Surface", Physical Review Letters, Vol. 30, No. 4, pp. 139-142, 22 January 1973.

Ashkin, A., "Atomic-Beam Deflection by Resonance-Radiation Pressure", Physical Review Letters, Vol. 25, No. 19, pp. 1321-1324, 9 November 1970.

Ashkin, A., "The Pressure of Laser Light", Scientific American, February 1972.

Cataneo, R., and Semonim, R. G., "Fall Velocities of Small Water Droplets in Still Air", Journal de Recherches Atmosphériques, Col. 4, No. 2, 1969.

May, A. D., Rawson, E. G., and Hara, E. H., "Propulsion and Angular Stabilization of Dust Particles in a Laser Cavity, II", Journal of Applied Physics, Vol. 38, No. 13, December 1967.

Rawson, Eric G., and May, A. D., "Propulsion and Angular Stabilization of Dust Particles in a Laser Cavity", Applied Physics Letters, Vol. 8, No. 4, 15 February 1966.

Stone, J., "Measurements of the Absorption of Light in Low-Loss Liquids", Journal of the Optical Society of America, Vol. 62, No. 3, March 1972.